FISEVIER

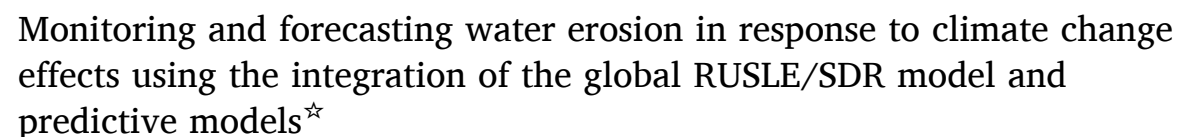
Contents lists available at ScienceDirect

## **Applied Soil Ecology**

journal homepage: www.elsevier.com/locate/apsoil



## Research paper





Belhaj Fatima <sup>a</sup>, Hlila Rachid <sup>a</sup>, Belkendil Abdeldjalil <sup>b</sup>, Ouallali Abdessalam <sup>c</sup>, Beroho Mohamed <sup>d</sup>, Alanoud T. Alfagham <sup>e</sup>, Aqil Tariq <sup>f,\*</sup>

- a Environmental Geology and Natural Resources Laboratory, University Abdelmalek Essaadi, Faculty of Sciences, Tétouan, Morocco
- <sup>b</sup> Centre de Recherche en Aménagement du Territoire (CRAT), Campus Zouaghi Slimane, Route de Ain el Bey, 25000, Constantine, Algérie
- c Process Engineering and Environment Laboratory, Faculty of Sciences and Techniques of Mohammedia, Hassan II University of Casablanca, Morocco
- d Geosciences Research and Development Laboratory, Department of Earth Sciences and Environment, Faculty of Sciences and Techniques of Al Hoceima (FSTH), Abdelmalek Essaädi University, Tetouan, Morocco
- <sup>e</sup> Department of Botany and Microbiology, College of Science, King Saud University, P.O. Box 2455, Riyadh 11451, Saudi Arabia
- f Department of Wildlife, Fisheries and Aquaculture, College of Forest Resources, Mississippi State University, Mississippi State 39762-9690, MS, USA

#### ARTICLE INFO

#### Keywords: Climate change Water erosion RUSLE/SDR Modeling Remote sensing and GIS

#### ABSTRACT

This study proposes a comprehensive concept and a novel approach to examine and assess the impact of climate change on soil degradation within the Loukkos watershed. The main aims of this study are to quantify and predict the potential rate of soil erosion, monitor its changes, and determine the sediment yield (SY) from 1999 to 2040 more accurately. This is achieved using the Revised Universal Soil Loss Equation (RUSLE), which accounts for variations in rainfall erosivity and soil cover, along with the linear mixed-effects model and Cellular Automata-Markov forecasting models and the Sediment Delivery Ratio (SDR). Our approach is based on data provided by remote sensing as well as daily rainfall data recorded at ten stations and multi-temporal time series satellite data for the reference period of 1999-2019. The results of the study revealed that soil erosion rates in the Loukkos basin range from 0 to 3797.66 t.ha<sup>-1</sup>.year<sup>-1</sup> between 1999 and 2040, with an average loss of 111.51  $t.ha^{-1}.year^{-1}$  and a SDR of 21.2 %. The average SY estimated by RUSLE/SDR is 6.81  $\mathrm{Mm}^3$ , almost equal to the value measured at the El Makhazine dam reservoir by the Loukkos Hydraulic Basin Agency (ABHL). We obtained detailed and reliable estimates showing that the average soil loss in 1999 was 100.64  $t.ha^{-1}.year^{-1}$ ; in 2009, it was 138.27  $t.ha^{-1}.year^{-1}$ , in 2019, it was 110.98  $t.ha^{-1}.year^{-1}$ , and it is projected to be 103.50  $t.ha^{-1}.year^{-1}$  in 2029 and 104.16 t.ha<sup>-1</sup>.year<sup>-1</sup> in 2040. This study will provide valuable concepts and insights into soil degradation in the study area, serving as a fundamental reference for researchers in this field. Additionally, it will be an essential guide for regional policymakers in planning soil erosion control strategies and watershed management.

#### 1. Introduction

Soil degradation is a form of loss of the fundamental properties of soil under the influence of natural and anthropogenic factors (Jie et al., 2002), such as rainfall patterns, topography, land use, and soil characteristics. These are the main determining factors that directly or indirectly lead to the activation of erosion processes and the increase in soil

erosion rates, threatening the components and management of watersheds (Chuenchum et al., 2020; Yan et al., 2023). Water erosion is a major phenomenon responsible for soil degradation and loss, detaching, transporting, and depositing soil particles from one area to another (Kidane et al., 2015). Most of the world's lands are experiencing a rapid increase and development of this serious problem, especially in the Mediterranean basin region, known as the epicenter of climate change

E-mail address: at2139@msstate.edu (A. Tariq).

https://doi.org/10.1016/j.apsoil.2025.105910

 $<sup>^{\</sup>star}$  This article is part of a special issue entitled: Soil Health II-ADV & CHLG published in Applied Soil Ecology.

<sup>\*</sup> Corresponding author.

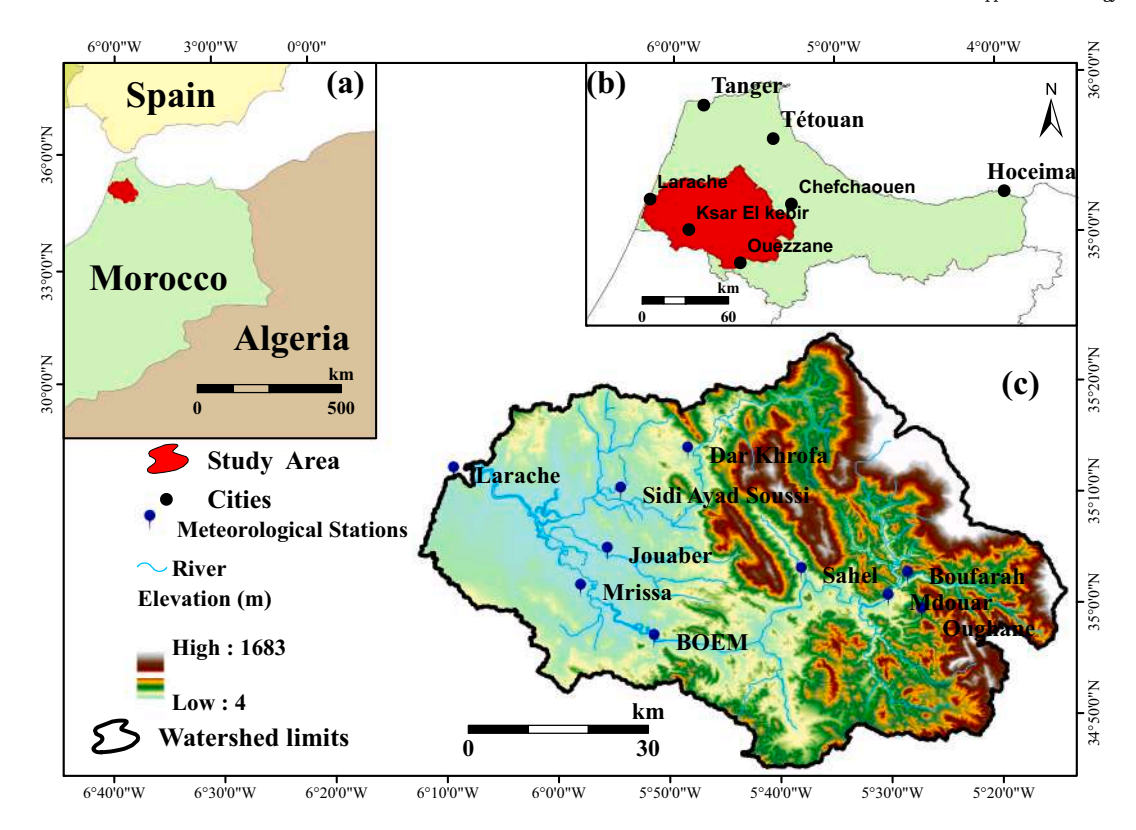


Fig. 1. Geographical location of the study area map; (a) Study area explained in the country, (b) study area with provincial boundary, (c) Study area with elevation and meteorological stations.

(Daliakopoulos et al., 2017; Werrell and Femia, 2017). Morocco, being one of the countries in this basin, faces this threat in many of its regions, particularly the Rif Mountains in northern Morocco, characterized by their steep slopes and highly erodible soils, with abundant and irregular rainfall (Vianney Nsabiyumva et al., 2023).

Soil erosion leads to severe imbalances in terrestrial ecosystems, significantly reducing agricultural yields and overall nutrition (Chen et al., 2024; Derpsch et al., 2024). Natural resources such as water and soil undergo degradation, affecting their components and physical properties (such as phosphorus, potassium content, organic carbon, nitrogen, and mineral and nutrient reserves), reducing root depth, available water, soil acidity, and fertility. Furthermore, water bodies downstream from erosion are rich in pesticide and fertilizer residues and contain large amounts of sediments (Bijay- and Craswell, 2021), which impede the natural flow of water, causing flooding and contaminating surface and groundwater.

To reduce the risk of this phenomenon, many scientists specialized in this field have identified and modified various models, linking them to Geographic Information Systems (GIS) and advanced remote sensing technologies to model and identify erosion sites and assess and measure soil erosion rates (Belhaj et al., 2024). Among these models are the Universal Soil Loss Equation (USLE) and its improved versions, the Modified Universal Soil Loss Equation (MUSLE) (Shi et al., 2022) and the Revised Universal Soil Loss Equation (RUSLE) (Eniyew et al., 2021), as well as other models like Soil and Water Assessment Tool (SWAT) (Abdelwahab et al., 2018; Cui et al., 2024) and Emergency Preparedness and Management (EPM) (Bezak et al., 2024), which are used in numerous studies of water erosion in watersheds worldwide, including Morocco.

One of the advantages of remote sensing (RS) and GIS is the ability to accurately and qualitatively monitor the spatio-temporal changes of specific phenomena on Earth (Vavassori et al., 2024; Zhang et al., 2024). In this study, we apply the coupled RUSLE/SDR model to monitor and assess the risk of soil erosion and estimate their expected average annual

loss and sediment yield (SY) in the Loukkos watershed in northwestern Morocco. This model was chosen because it is based on various satellite images and geospatial analyses, utilizing RS and one of the GIS software packages. It is considered one of the most successful and widely used models due to its simplicity and data availability, making it widely accepted by the soil erosion community. The average annual soil loss (A) is the product of five factors multiplied together within ArcGIS 10.4.1 software, namely Rainfall erosivity (R), soil erodibility (K), slope length and steepness (LS), cover management (C), and support practices (P).

In the context of soil erosion monitoring and forecasting, numerous studies have been conducted worldwide, examining soil erosion in relation to future changes in climate and/or land use, including: Europe (Panagos et al., 2021), Morocco (North Africa) (Alitane et al., 2022; Ammari et al., 2023; Bammou et al., 2024), Ethiopia (Getachew et al., 2021), China (Jin et al., 2021), Iran (Sardari et al., 2019), Spain (Eekhout and De Vente, 2020) and Thailand (Plangoen et al., 2013). In most of these studies, the authors emphasize that the projected increase in soil loss will mainly be driven by the anticipated rise in rainfall erosivity, with climate change being the primary factor (Borrelli et al., 2020; Du et al., 2024). However, other studies suggest that changes in land use will be responsible for increased soil erosion in the future (Jazouli et al., 2019; Paroissien et al., 2015). For these reasons, it is recommended to assess the current and future impacts of climate change and land use on soil loss (Panagos et al., 2021; Sardari et al., 2019) to better protect land and water resources at the watershed scale (Girmay et al., 2021).

However, we found that most studies on soil erosion worldwide, for example Algeria (Saoud and Meddi, 2023), Tunisia (Serbaji et al., 2023), Ethiopia (Yeneneh et al., 2022), Taiwan (Liou et al., 2022), South-Central Niger (Almouctar et al., 2021), and more specifically in Morocco (Acharki et al., 2023; Bassairate et al., 2021; Ouallali et al., 2016; Tahiri et al., 2017), focus solely on historical or current conditions, without considering the future impacts of climate change and land use on soil erosion (Jazouli et al., 2019; Simonneaux et al., 2015). This is

one of the reasons why we decided to conduct this study in our region.

Based on the research conducted in this study, none of the previous studies have provided comprehensive and reliable projections of soil loss that could occur in coming years due to the impact of future changes in precipitation and vegetation in a specific region of Morocco. The novelty of this study lies in utilizing the Linear Mixed-Effects (LME) model and the Cellular Automata/Markov (CA-Markov) model to predict precipitation and NDVI, which are used to estimate the R and C factors of the RUSLE equation.

In this context, this study introduces a comprehensive concept and a novel approach to investigate and assess the effects of climate change and land cover on soil erosion in the Loukkos watershed in northwest Morocco. The specific objectives of this paper are: (i) to quantify and more accurately predict the potential soil erosion rate using the RUSLE, considering future changes in erosivity and land cover (R and C factors), and to monitor their trends over the period 1999–2040; (ii) to identify areas that will be vulnerable to soil erosion; and (iii) to evaluate the average SY using the coupled RUSLE-SDR model. The results will undoubtedly provide important and useful insights and serve as a valuable reference for policymakers in planning the necessary strategies to mitigate and reduce this hazardous phenomenon.

#### 2. Materials and methods

#### 2.1. Study area

The Loukkos watershed is located in northwestern Morocco, between  $6.20^{\circ}$  and  $5.24^{\circ}$  west longitude and  $34.75^{\circ}$  and  $35.40^{\circ}$  north latitude (Fig. 1a). It covers an area of  $3743.46~\rm km^2$  and has a perimeter of  $376.76~\rm km$ . Its principal cities are Larache, Ksar el-Kebir, and Ouazzane (Fig. 1b). The climate is semi-humid, with average annual precipitation ranging from approximately 700 mm to 1014 mm. Light rainfall is recorded in the western part of the flat plain of the Loukkos Valley, which reaches a minimum altitude of 4 m. In contrast, heavy rainfall has been recorded in the eastern part of the basin, at high altitudes, reaching a maximum value of  $1683~\rm m$  (Fig. 1c).

From a hydrological perspective, the Loukkos River is considered the main river of the watershed and one of the most important rivers in Morocco in terms of flow and associated agricultural and economic activities (Hrour et al., 2023). It originates at Jbel El Khzana in the province of Chefchaouen, at an altitude of over 1600 m. It flows for 180 km westward to the mouth of the Atlantic Ocean near the city of Larache. Its tributaries include the Oued Ouarour (200 km<sup>2</sup>) and the Oued El Makhazine (880 km<sup>2</sup>). Its hydrology is closely linked to rainfall conditions and exhibits significant interannual irregularities. The watershed also contains three major dams: the Oued El Makhzen dam, with a capacity of 782 m<sup>3</sup>, serves to provide drinking water, generate hydroelectricity, rinse, and reduce flood risks. The Dar Khrofa dam, with a storage capacity of 480 m<sup>3</sup>, is also used for irrigating agricultural land and is connected to Tangier's drinking water supply system. Additionally, the Gard Dam aims to raise the river's water level to facilitate irrigation pumping and protect the downstream valley from seawater intrusion.

Its climate and geomorphological structure endow the basin with significant hydrological potential, contributing to the development of irrigated agricultural activities in the area and making it one of the most important agricultural regions in Morocco (Abbou et al., 2023). Consequently, agriculture is considered the main economic activity of the basin, as the available agricultural area represents 57 % of the basin's total area, with 21 % covered by irrigated agriculture and the remainder by rain-fed agriculture (Ahmed et al., 2021). It is noteworthy that the Regional Office for Agricultural Development of Loukkos (ORMVAL) is responsible for agricultural development within the basin. At the same time, the Hydraulic Basin Agency of Loukkos (ABHL) oversees the distribution and management of hydraulic infrastructures (dams and irrigation).

Table 1
Datasets were used in this research.

Data sets	Resolution	Associated Factor	Data Source
Precipitation data		R	Hydraulic Basin Agency of Loukkos (ABHL) (http://www.abhloukkos. ma)
Soil data		K	Food and Agriculture Organization (FAO) www.fao.org/geonetwork/s rv/en/metadata.show? id=14116&currTab=d istribution)
Soil map			https://edepot.wur.nl/487491
DEM	30 m	LS	Earthexplorer.usgs.gov
Landsat 4–5 and 8	30 m	С	USGS Earth Explorer/ Earthexplor er.usgs.gov

#### 2.2. Datasets

We used the data to conduct the research described in Table 1 below.

#### 2.2.1. Precipitation data

The precipitation data used in this work are daily records from 1999 to 2019 from ten stations in the study area provided by the Hydraulic Basin Agency of Loukkos (ABHL) (Table 1). A mixed-effects model is then used via R software to predict future precipitation, determine the erosivity factor (R), and assess hydrological responses under climate change scenarios.

#### 2.2.2. Soil data

We used the World Digital Soil Map (DSMW) database (Table 1) to identify the main soil types in the Loukkos region and extract their properties. We then verified the accuracy of the obtained data using a soil-type distribution map of Morocco at a scale of 1:2,000,000 established by the mapping department of the Moroccan Directorate of Cadastre and Mapping (Table 1). Consequently, we used this data to estimate the erodibility factor (K).

## 2.2.3. Digital elevation model (DEM)

The  $30\ m\ x\ 30\ m$  digital elevation model was downloaded from the US Geological Survey website (Table 1) to extract the slope length (L) and slope steepness (S), to determine the LS erosion factor using ArcMap extensions.

## 2.2.4. Satellite images

In this study, we used satellite images taken in spring (the plant blooming season), characterized by low cloud cover (<10 %), to extract vegetation index maps. Consequently, we selected the Landsat 4–5 TM C1 Type 1 level 1 image dated May 24, 1999, May 3, 2009, and the Landsat 8 image dated May 15, 2019 (Table 1). The CA-Markov simulation model is then used to predict future NDVI values closely reflecting reality to assess vegetation responses under climate change scenarios, thereby determining the current and expected cover management factors (C).

## 2.3. Methodology

The estimation and prediction of soil loss during the study period are based on applying the RUSLE on the LME and CA-Markov prediction models and the SDR. The methodology developed in this research is presented in Fig. 2.

## 2.3.1. RUSLE equation

The application of the RUSLE eq. (1) to estimate the average soil loss (A) requires the preparation of several maps of the different factors, namely rainfall erosivity (R), soil erodibility (K), slope length and steepness (LS), cover management (C), and support practices (P) (Wischmeier and Meyer, 1973):

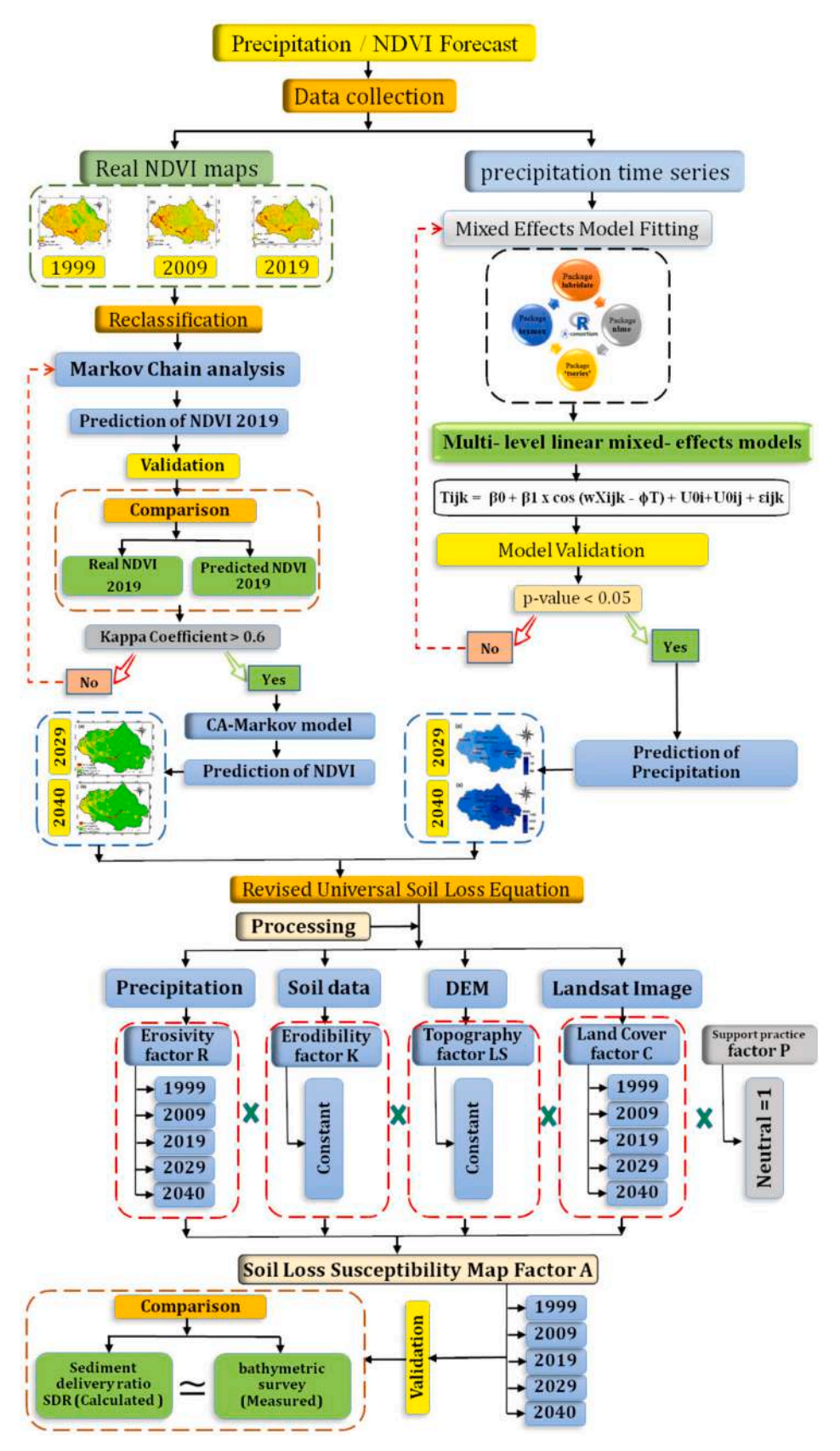


Fig. 2. Methodology applied in the study.

**Table 2**Monitoring and prediction of annual average rainfall and R Factor of Loukkos watershed.

Station	Coordinates		1999		2009		2019		2029		2040	
Name	Lat.	Long.	Average Rainfall (mm)	R (MJ mm ha $^{-1}$ h $^{-1}$ year $^{-1}$ )	Average Rainfall (mm)	R (MJ mm ha $^{-1}$ h $^{-1}$ year $^{-1}$ )	Average Rainfall (mm)	R (MJ mm ha <sup>-1</sup> h <sup>-1</sup> year <sup>-1</sup> )	Average Rainfall (mm)	R (MJ mm ha <sup>-1</sup> h <sup>-1</sup> year <sup>-1</sup> )	Average Rainfall (mm)	R (MJ mm ha <sup>-1</sup> h <sup>-1</sup> year <sup>-1</sup> )
BOEM	34.94	-5.85	319.6	520.4	891.3	2734.8	600.8	1437.8	355.9	618.9	457.1	925.9
Oughane	34.98	-5.45	355.6	618.0	1209.0	5077.2	868.8	2603.8	442.3	878.0	577.7	1349.9
Mdouar	35.00	-5.50	387.7	710.3	1233.1	5288.7	681.9	1762.9	202.9	250.4	190.9	227.0
Mrissa	35.02	-5.96	319.6	520.4	927.6	2960.5	533.8	1188.6	354.0	613.4	413.8	788.8
Boufarah	35.03	-5.47	424.4	821.6	1433.6	7233.1	739.9	2010.6	572.4	1329.9	609.1	1469.9
Sahel	35.04	-5.63	605.0	1454.0	1450.2	7408.8	784.7	2210.1	519.4	1137.3	599.2	1431.6
Jouaber	35.07	-5.92	293.4	453.5	451.1	906.4	395.1	732.2	275.0	408.6	309.8	495.0
Sidi Ayad	35.16	-5.90	300.2	470.5	974.0	3264.6	611.5	1479.3	362.5	637.6	442.0	877.3
Soussi												
Larache	35.19	-6.15	294.5	456.2	991.4	3383.4	445.3	887.7	363.1	639.2	393.7	728.1
Dar Khrofa	35.22	-5.80	345.4	589.7	1145.6	4543.5	710.0	1881.4	692.0	1805.2	741.1	2015.7
Average			364.5	661.5	1070.7	4280.1	637.2	1619.4	413.9	831.8	473.4	1030.9

$$A = R \times K \times LS \times C \times P \tag{1}$$

Where: (A) is the average soil loss  $(t.ha^{-1}.year^{-1})$ ; (R) is the rainfall erosivity factor  $(Mj. Mm/h.ha^{-1}.year)$  (K) is the soil erodibility factor  $(Mj. Mm/h.ha^{-1}.year)$ ; (LS) is the topographic factor representing slope length (L in meters) and steepness (S in %), (dimensionless); (C) is the cover management factor (ranging from 0 to 1, dimensionless); (P) is the factor for anti-erosive support practices (ranging from 0 to 1, dimensionless).

#### a) Erosivity Factor (R)

The R factor represents the potential soil loss due to precipitation. This has led many researchers to propose various empirical models to estimate this factor based on daily, monthly, and annual precipitation (Lee and Lin, 2015). In this article, this factor is evaluated using the eqs. (2) and (3) (Renard and Freimund, 1994).

$$R = 0.0483 * P^{1.610} \text{ if } P \le 850 \text{ mm}$$
 (2)

$$R = 0.004105 \times P^2 - 1.249 \times P + 587 \text{ if } P > 850 \text{ mm}$$
 (3)

Where: P is the average annual precipitation (mm).

The satellite images on which we based this study date back to May. Hence, the precipitation that directly affects the vegetation cover in that month comes from the rainfall received in autumn, winter, and spring. This led us to sum the precipitation from the months of these three seasons for each year 1998–1999 to 2039–2040 at each station and then calculate their averages (Table 2).

Consequently, the R factors were calculated based on these point precipitation data using the previous eqs. (2) and (3) and were interpolated throughout the studied watershed using the IDW interpolation method in ArcGIS version 10.8.1.

## ✓ Precipitation Forecasts

To predict future precipitation, we used a "new" two-level mixed effects model: level (1) represents the months, and level (2) represents the years (Beroho et al., 2020), developed using the statistical software "R" version 3.6.2 (R Core Team, 2017), and adapted with the "nlme" library (Pinheiro and Bates, 2006). This model is based on daily data from 1999 to 2019 from 10 rainfall stations. By applying the following eq. (4)(Beroho et al., 2020):

$$T_{ijk} = \beta_0 + \beta_1 * cos \left( wX_{ijk} - \varphi T \right) + U_{0i} + U_{0ij} + \varepsilon_{ij}$$

$$\tag{4}$$

Where: i is the index of the month's observations. j is the index of the year observations.  $T_{ijk}$  is the k-th observation of precipitation for a

**Table 3** Precipitation (mm) adjustment summary.

Fixed effect	Estimation	Estimation					
	Value	Std. error	p-Value				
β0	2.2125	0.4828	0.0000				
β1	0.2822	0.1152	0.0144				

Random Effect	Value	
σb0(i) σb0(i)j	1.6116 1.5911	
$\sigma\Sigma$	7.1353	

month (i) of the year (j).  $\beta_0$  is the average precipitation of a month at time zero.  $\beta_1$  is the average increase in precipitation over time.  $U_{0i}$  is the random effect specifying the month (i) at the intercept  $\beta$ 0.  $U_{0ij}$  is the random effect specifying the year (j) including the associated month (i) at the intercept  $\beta$ 0 (Table 3).

## b) Erodibility Factor (K)

The factor (K) determines the soil's ability to resist erosion. It depends on the physical and chemical properties of the soil, as well as the intensity and kinetic energy of precipitation. In this study, the value of the factor K is calculated using the eq. (5) proposed by Tsige et al. (2022). Based on the data extracted from the FAO soil map, the downloaded "DSMW" file provides all the information for each layer in shapefile and Excel format. The results of the equation are presented in **Supplementary Table 1**.

$$K_{usle} = f \, csand \times f \, cl - si \times f \, oragC \times f \, his and \tag{5}$$

$$fcsand = \left(0, 2+0, 3 \times EXP \left[-0, 256 \times ms \times \left(1 - \frac{msilt}{100}\right)\right]\right) \tag{6}$$

$$fcl - si = \left(\frac{msilt}{mc + msilt}\right)^{0.3} \tag{7}$$

$$foragC = \left(1 - \frac{0.25 \times orgC}{orgc + EXP(3.72 - 2.95 * orgC)}\right) \tag{8}$$

fhisand = 
$$\left( 1 - \frac{0.7 \left( 1 - \frac{ms}{100} \right)}{\frac{ms}{100} + EXP\left( -5.5 + 22.9 \times \left( 1 - \frac{ms}{100} \right) \right)} \right)$$
 (9)

Where ms being the percentage of sand (0.05-2.00 mm), msilt being

the percentage of silt (0.002–0.05 mm), mc being the percentage of clay (<0.002 mm), and orgC being the organic carbon content (SOC) (%).

#### c) Factor of Topography (LS)

The factor (LS) is a topographic index that represents the shape of the terrain. It considers the effects of the length (L) and slope (S) of the slope on the rate of surface runoff leading to water erosion. The longer and steeper the slope, the greater the erosion. To determine this factor, we used the eq. (10) developed by Sakhraoui (2023).

$$LS = \left(\frac{X}{22.1)^m} \cdot (0,065 + 0,045.S + 0,0065.S^2)\right) \tag{10}$$

Where; X is the length of the slope in meters, where  $X = (flow \ accumulation \times resolution)X = (\text{text}\{flow \ accumulation\} \times \text{text}\{resolution\})X = (flow \ accumulation \times resolution)$ . S is the slope percentage (Supplementary Fig. 1). Resolution: 30 m. m is a constant related to the slope, equal to 0.5, according to Supplementary Table 2 and Supplementary Fig. 1.

#### d) Vegetation Cover Factor (C)

The factor (C) reflects the impact of vegetation cover and cultivation techniques on soil erosion (Chalise et al., 2019). It is a spatio-temporal variable related to precipitation dynamics and plant growth (Yuan et al., 2022). The C factor is determined based on the NDVI using the eq. (11) developed by Durigon et al. (2014):

$$C = \left(\frac{-NDVI + 1}{2}\right) \tag{11}$$

The NDVI is a good indicator for monitoring vegetation activity. It is calculated using eq. (12). Its values range from -1 to 1, with high values representing green and dense vegetation, while low values indicate bare land or water bodies.

$$NDVI = \frac{(PIR - R)}{(PIR + R)} \tag{12}$$

Where: PIR is the reflectance in the near-infrared band, and R is the reflectance in the red band.

#### ✓ NDVI Forecasting

In this study, we applied the CA-Markov model from Idrisi Andes to predict the NDVI for 2029 and 2040 based on the NDVI from 1999, 2009, and 2019. The model combines CA-Markov processes to enhance the computational efficiency of the simulation (Cui et al., 2021; Nie et al., 2015). The NDVI for 2019 was predicted using the transition probability matrix between the different NDVI categories from 1999 to 2009. A Kappa accuracy test was conducted on the predicted data and the actual NDVI data from 2019 to verify the simulation results. Consequently, the NDVI for 2029 and 2040 is predicted based on the class transition probability matrix of the NDVI from 2009 to 2019 (Abdelkarim, 2023).

## e) Factor of Erosion Control Practices (P)

The factor P reflects the effectiveness of measures aimed at reducing runoff velocity and preventing soil erosion (Panagos et al., 2015). The most significant supporting measures include contour farming, strip cropping, and terracing. The value of P ranges from 0 to 1, where 0 represents very effective erosion control practices, and 1 indicates no erosion control practices (J. Li et al., 2024).

## f) Estimation of Soil Loss Rate (A)

**Table 4**Estimation of sediment delivery from the Loukkos watershed, according to the model FPM

model 21 mi	
Surface (km <sup>2</sup> )	3743.46
Surface (mil <sup>2</sup> )	2326.08
Perimeter	376.7
length of the main water course (km)	124
Maximal length of the watershed inferred parallel to the mainstream (km)	88
Maximum altitude	1683
Minimum altitude (m)	4
R: watershed relief $=$ maximum height of the watershed $-$ outlet elevation	1679
Outlet height (m)	4
Mean elevation (m)	271.71
D (km)	0.26771
EPM (Ru)	0.40988689

The spatial distribution of soil loss (factor A) is estimated and mapped based on the product of the five factors described above, following the empirical equations of the RUSLE model in ArcGIS 10.4.1, using the option Spatial Analyst Tools > Map Algebra > Raster Calculator. To facilitate the analysis and identification of erosion severity levels in the Loukkos watershed, each estimated soil loss map has been divided into the following five categories (Fig. 8):

#### 2.4. Validation

The SDR represents the total amount of soil lost and transported downstream from a specific area over a defined time period (Dos Santos et al., 2017). At the watershed level, this ratio can be determined by comparing the sediment generated within erosion-prone areas to the sediment discharged through the watershed outlet (Puno et al., 2021). In practice, the proposed equations apply only to lands influenced by the primary factors for which they were developed. We included all nine SDR parameters involved in the process to fully assess the capability of our models (Supplementary Table 3) (Xu et al., 2024). We then used the Ru ratio to identify the most suitable model, considering comparative methods, standard error (SE), and the coefficient of variation (Boufeldja et al., 2020).

The resulting SDR values (**Supplementary Table 3**) vary across models depending on the factors incorporated into each model. For comparison, we calculated the sediment-output ratio "Ru" for the EPM model using Eq. 13.

$$Ru = \frac{4(P \times D)^{0.5}}{L + 10} \tag{13}$$

Where Ru represents the sedimentation coefficient of the watershed, L is the length of the line connecting both ends of the watershed (in km), P is the watershed perimeter, and D is the topographic difference between the average elevation and the lowest elevation of the watershed, defined as  $D=D_{ar}$  -  $D_{o}$ , with  $D_{o}$  being the elevation (in km) at the watershed outlet. Consequently, the sediment-output ratio Ru is calculated as 0.40988689 (as shown in Table 4).

To identify the most suitable model for our study area, we employed multiple approaches, including adaptive comparisons, the coefficient of variation (CV), standard deviation, and standard error (SE) (Belkendil et al., 2016), as outlined in Eqs. (14–16).

$$CV = \frac{SD}{X_0} \times 100 \tag{14}$$

$$SD = \sqrt{\frac{(X_e - X_0)^2}{X_0}} \tag{15}$$

$$SE = \frac{\left| (SDR)_E - (SDR)_B \right|}{(SDR)_E} * 100 \tag{16}$$

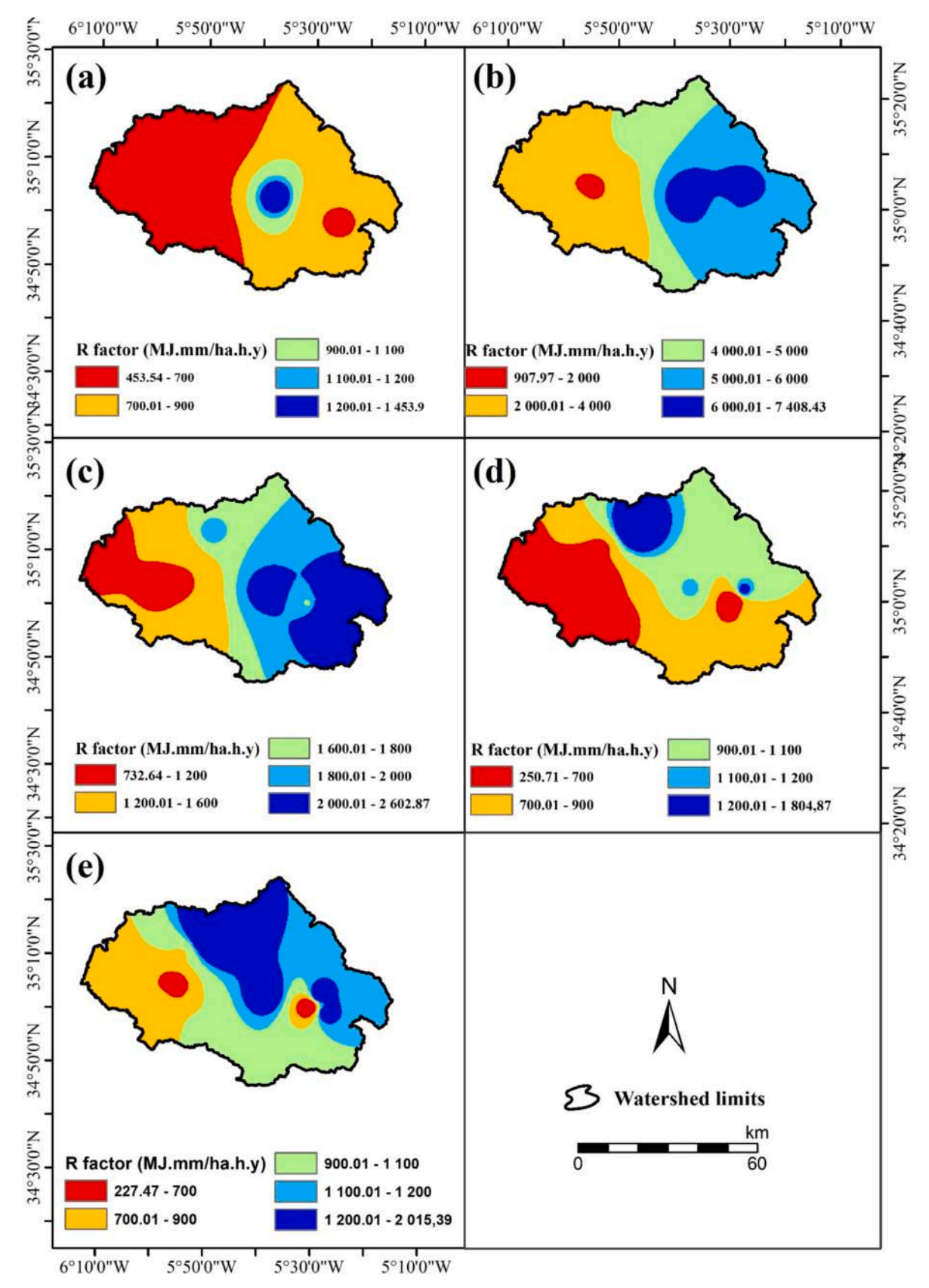


Fig. 3. Spatial distribution of erosivity (R) for Loukkos watershed. (a) 1999, (b) 2009, (c) 2019, (d) 2029, and (e) 2040.

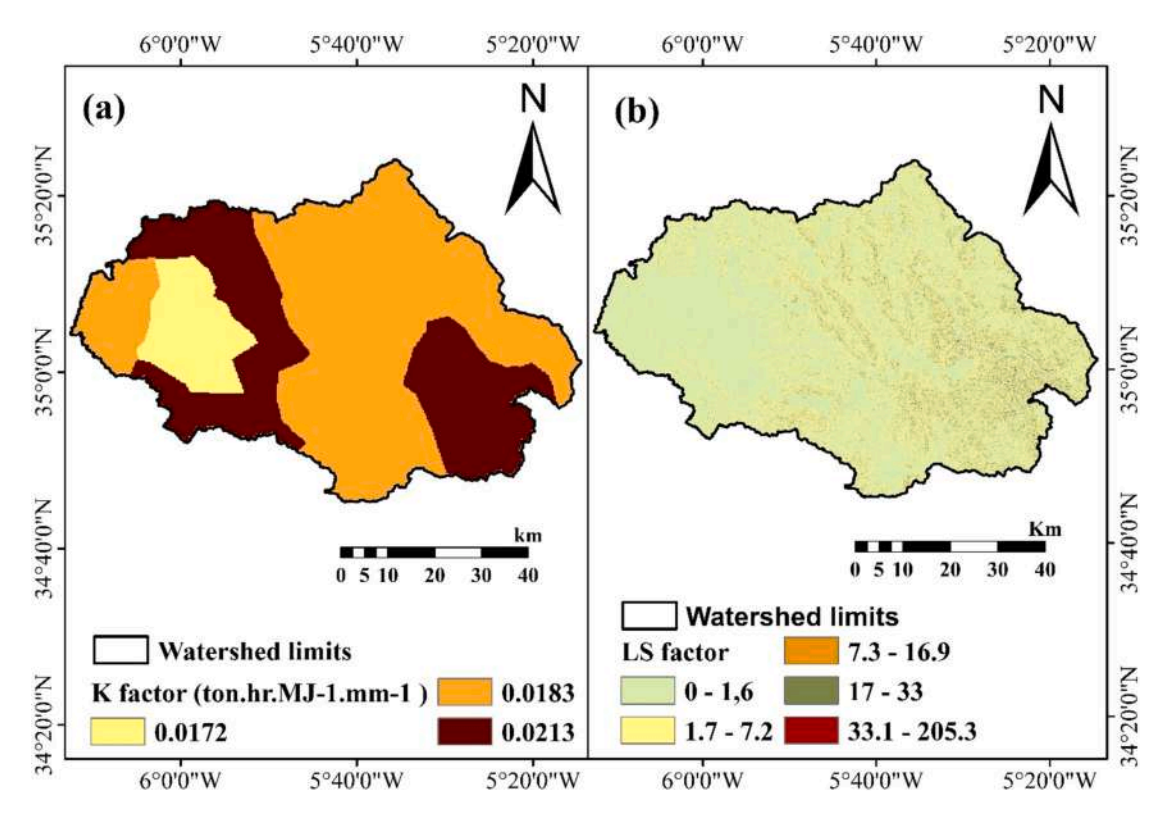


Fig. 4. Spatial distribution of RUSLE parameters: (a) K-factor; (b) LS-factor.

Where CV is the coefficient of variation; SD is the standard deviation;  $X_0$  is the observed SDR  $(SDR_0)$ ;  $X_e$  is the estimated SDR  $(SDR_e)$ ;  $SDR_B$  is the sediment delivery rate.

## 3. Results

## 3.1. Analysis of factor maps

## a) Erosivity Factor (R)

We simulated future precipitation projections up to 2040 using a linear mixed-effects model (LME) based on daily precipitation data from 1999 to 2019. The validity and accuracy of the precipitation forecast simulations are indicated by a *p*-value lower than 0.05 (see Table 3). Therefore, the standard deviation values for the fixed and random effects are very low. Additionally, the amounts of precipitation and the errors align well with the fitted values (Supplementary Fig. 2).

The satellite images on which we based this study date back to May. Hence, the precipitation that directly affects the vegetation cover in that month comes from the rainfall received in autumn, winter, and spring. This led us to sum the precipitation from the months of these three seasons for each year of 1998/1999 to 2039/2040 at each station and then calculate their averages (Table 2).

Consequently, the R factors were calculated based on these point precipitation data using the previous eqs. (2) and (3), and were interpolated throughout the studied watershed using the IDW interpolation method in ArcGIS version 10.4.1, as shown in Figs. 3a, b, c, d, and e. The results indicate that the values of the R factor are high, ranging from 227.47 to 7408.43 (*Mj. Mm/h.ha*<sup>-1</sup>.year) (Fig. 3), with an overall average of 1684.76 (*Mj. Mm/h.ha*<sup>-1</sup>.year), specifically 661.47 (*Mj. Mm/h.ha*<sup>-1</sup>.year)in 1999, 4280.11 (*Mj. Mm/h.ha*<sup>-1</sup>.year) in 2009, 1619.44 (*Mj. Mm/h.ha*<sup>-1</sup>.year) in 2019, and 831.84 (*Mj. Mm/h.ha*<sup>-1</sup>.year) in 2029, and 1030.92 (*Mj. Mm/h.ha*<sup>-1</sup>.year)in 2040 (Table 2), indicating a significant variation between years due to changes in

**Table 5**Class distribution of factor K throughout the Loukkos watershed.

Soil of Loukkos	factor K (Mj. Mm/h.ha <sup>-1</sup> .year)	Area	Percentage
watershed		(km²)	(%)
Eutric Fluvisols (Je) Carbonate Kastamozems (Kk)	0,0172	368,32	9,88
	0,0213	1203,09	32,27
Chromatic Luvisols (Lc)	0,0183	2157,31	57,86

precipitation during this period. Thus, the highest value occurred in 2018/2019, with a maximum average rainfall of 1070.69 mm, while the lowest was recorded in 1998/1999, with a minimum average rainfall of 364.54 mm. It is observed that precipitation strongly impacts changes in erosivity and, consequently, on soil loss. The highest values are primarily recorded in the eastern part of the basin, whereas the lowest values are recorded downstream of the basin (Fig. 3).

## b) Factors of Erodibility (K) and topography (LS)

Fig. 4a illustrates the spatial distribution of the erodibility factor K in the Loukkos watershed, with values ranging from 0.0172 to 0.0213 ( $Mj. Mm/h.ha^{-1}.year$ ). The highly erodible soils are Kastamozems calciques (Kk), which account for 32.27 % of the area, followed by Luvisols chromiques (Lc), characterized by moderate erodibility and covering more than half of the watershed area (57.86 %). In contrast, the least erodible soils are Fluvisols eutriques (Je), representing only 9.88 % of the total area (Table 5).

Fig. 4b shows the spatial distribution of LS factor values, ranging from 0 to 205.3. The lowest values are recorded in the plains and riverbeds of the watershed, while relatively higher values are associated with steeper slopes, particularly in the upper valleys and upstream areas, where the rugged topography is more susceptible to erosion processes (Ochoa et al., 2016). These higher values are concentrated in the eastern

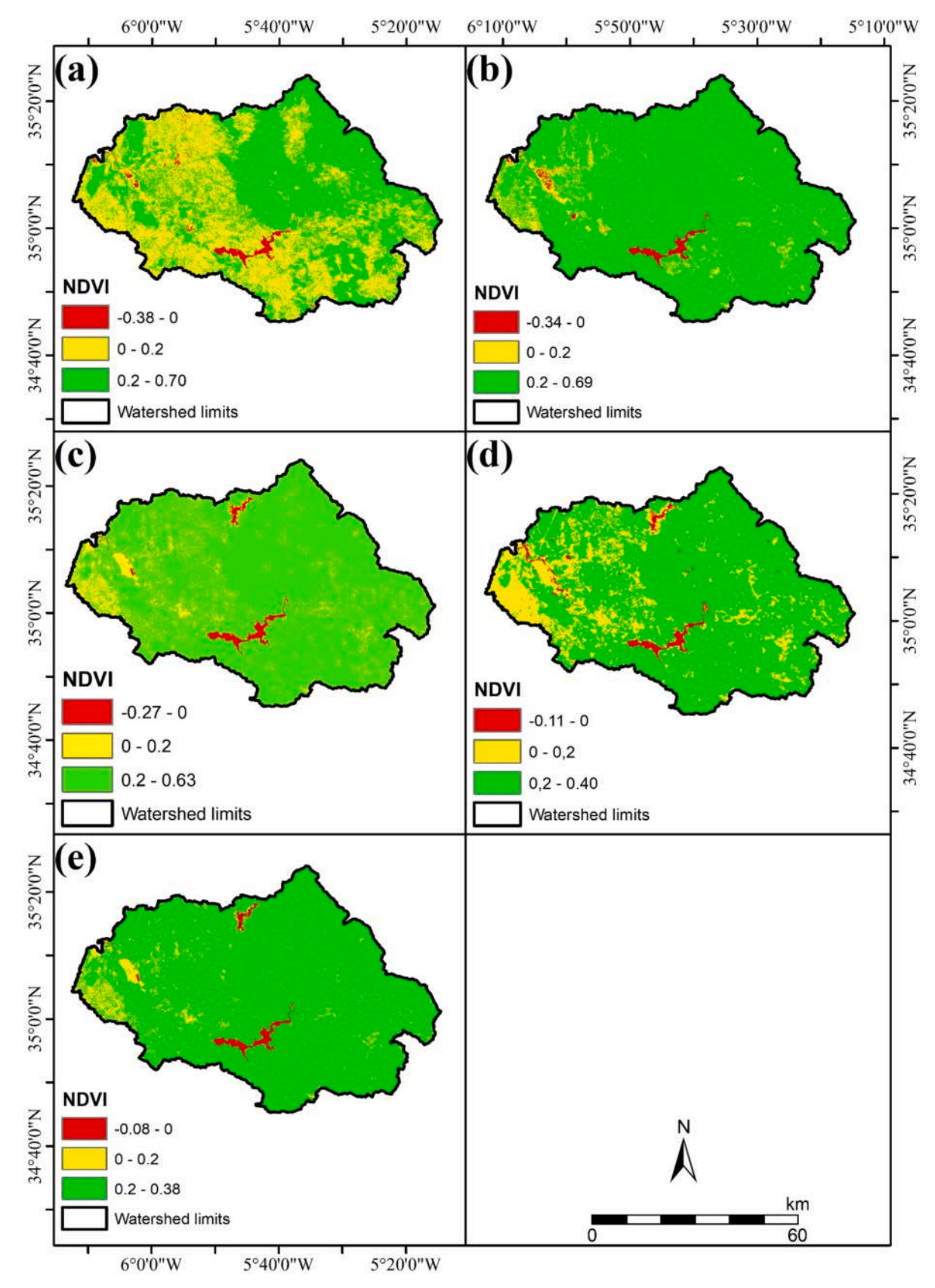


Fig. 5. Spatial distribution of the NDVI for Loukkos watershed. (a) 1999, (b) 2009, (c) 2019, (d) 2029, and (e) 2040.

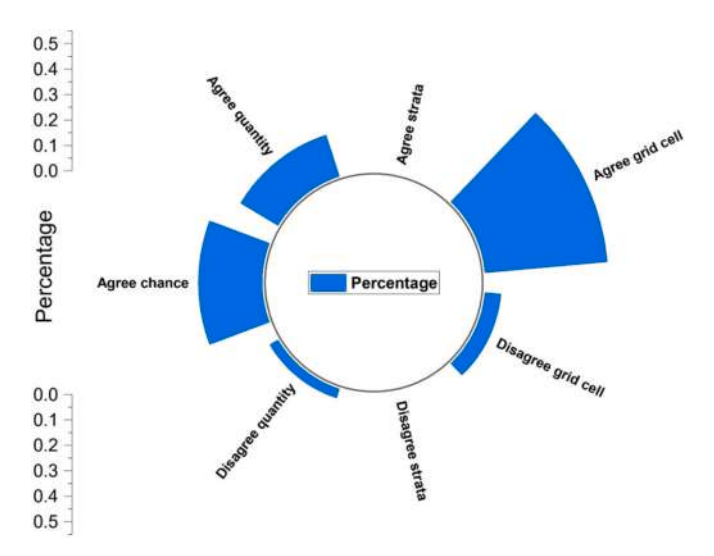


Fig. 6. Validation of CA-Markov model.

part of the watershed.

#### c) Factor of vegetation Cover (C)

Based on the NDVI data from 1999, 2009, and 2019, we used the CA-Markov model to obtain the NDVI for 2029 and 2040 (Fig. 5). The Kappa index values of the simulation results between the simulated NDVI 2019 map (Supplementary Fig. 3) and the actual one are Klocation = 0.88 (88 %), Kn0 = 0.86 (86 %), and Kstandard = 0.83 (83 %) (Fig. 6), indicating an almost perfect agreement between the two maps, and suggesting that the NDVI forecasts for 2029 and 2040 will be very close to reality.

The method for obtaining the factor (C) using the NDVI index assumes a linear relationship between them. The results of this study revealed a strong negative correlation, with the R<sup>2</sup> coefficient during the study period reaching 0.9948 (**Supplementary Fig. 4**). This indicates that the two variables tend to move in opposite directions. As factor C decreases, the NDVI value increases, indicating good protection and conservation of land cover, and vice versa (Figs. 5 and 7).

The obtained factor (C) maps (Fig. 7) show that the distribution of its values is quite heterogeneous throughout the area. This value difference (C) reflects the variation in vegetation cover density within the watershed (Table 6). Values of  $C \le 0.3$  indicate that vegetation cover is well developed and the soil is well protected. In contrast, values of C > 0.3confirm poor soil protection in urban areas, agricultural lands, shrublands, grasslands, and lands exposed to heavy rainfall and completely bare soils. These are mainly distributed in the western and eastern parts of the basin, characterized by low vegetation cover due to significant urban expansion and agricultural activities primarily conducted on plains with fertile alluvial deposits. However, urban expansion and population growth have led to the emergence of rural areas in the Loukkos basin, with a total estimated population of 861,188 people (Supplementary Fig. 5), and subsistence agriculture in steep areas, resulting in deforestation and thereby exacerbating the risk of erosion. The spatial distribution of factor C confirms that human activities related to land use and climate change have long affected the area, leading to forest degradation and conversion into cultivated lands, steppes, and pastures (De Chazal and Rounsevell, 2009).

## d) Factor of Erosion Control Practices (P)

Most farmers in the Loukkos Basin do not implement the erosion control measures recommended by agricultural experts. Most crops in the basin are cereals, which are rarely grown parallel to the contour lines

of the basin. For these reasons, we assign a value of 1 to the factor P for the entire watershed area. It is also for these reasons that most studies conducted in Morocco have adopted this value (El Assaoui et al., 2023).

#### 3.2. Estimation of soil loss rate

The spatial distribution of soil loss (factor A) is estimated and mapped based on the product of the five factors described above, following the empirical equations of the RUSLE model in ArcGIS 10.4.1, using the option Spatial Analyst Tools > Map Algebra > Raster Calculator. To facilitate the analysis and identification of erosion severity levels in the Loukkos watershed, each estimated soil loss map has been divided into the following five categories (Fig. 8):

Based on the resulting soil loss maps over the period (1999–2040), each pixel in the total area of the Loukkos basin (3743.46 km²) has a value corresponding to its erosion potential, with an overall range of 0 to  $3797.66 \ t.ha^{-1}.year^{-1}$  and an average rate of  $111.51 \ t.ha^{-1}.year^{-1}$ .

The results in Table 7 show that the average soil loss in 1999 was  $100.64\ t.ha^{-1}.year^{-1}$ . In 2009, it was  $138.27\ t.ha^{-1}.year^{-1}$  in 2019, it was  $110.98\ t.ha^{-1}.year^{-1}$ , and it is expected to reach  $103.50\ t.ha^{-1}.year^{-1}$  in 2029 and  $104.16\ t.ha^{-1}.year^{-1}$  in 2040. Thus, the lowest average recorded during this period was in 1999, while the highest was recorded in 2009. It is noted that the average annual soil loss significantly increased by  $+37.39\ \%$  (from  $100.64\ to\ 138.27\ t.ha^{-1}.year^{-1}$ ) from 1999 to 2009 and then decreased by  $-19.74\ \%$  (from  $138.27\ to\ 110.98\ t.ha^{-1}.year^{-1}$ ) from 2009 to 2019, and it will further decrease by  $-6.75\ \%$  (from  $110.98\ to\ 103.50\ t.ha^{-1}.year^{-1}$ ) from 2019 to 2029, while there will be a slight increase of  $+0.64\ \%$  (from  $103.50\ to\ 104.16\ t.ha^{-1}.year^{-1}$ ) from 2029 to 2040.

This study set the soil erosion tolerance threshold at  $25 \ t.ha^{-1}.year^{-1}$ . Therefore, areas where soil erosion rates exceed  $25 \ t.ha^{-1}.year^{-1}$  are considered highly eroded and require urgent measures to prevent and control soil erosion (Fig. 8). The analysis showed that the area with a soil erosion rate  $\leq 25 \ t.ha^{-1}.year^{-1}$  in the Loukkos watershed was estimated at approximately  $3451.90 \ km^2$  (92.21 %), 2928.80 km² (78.24 %), and  $3202.44 \ km^2$  (85.55 %) in 1999, 2009, and 2019, respectively. Meanwhile, in 2029 and 2040, the area will reach approximately  $3406.02 \ km^2$  (90.99 %) and  $3327.34 \ km^2$  (88.88 %), respectively. In contrast, the area with a soil erosion rate  $> 25 \ t.ha^{-1}.year^{-1}$  was estimated at approximately  $291.56 \ km^2$  (7.79 %) in 1999,  $814.66 \ km^2$  (21.76 %) in 2009, and  $541.02 \ km^2$  (14.45 %) in 2019. The area is expected to reach approximately  $337.44 \ km^2$  (9.01 %) in 2029 and  $416.12 \ km^2$  (11.12 %) in 2040 (Table 7).

In the Loukkos basin, areas with low soil loss values  $<25 \ t.ha^{-1}$ .  $year^{-1}$  are characterized by lower values of the LS, K, and R factors and the protective effect of vegetation. They are mainly concentrated in the western part of the basin, downstream and near the rivers, where the land is flat or gently sloped, with good irrigation conditions and high vegetation density, making them very resistant to erosion (Kosmas et al., 2000). In contrast, areas with erosion categories  $>25 \ t.ha^{-1}$ .  $year^{-1}$  are characterized by higher LS, K, and R values and lack vegetation. They are mainly distributed in the eastern part of the basin, where the terrain is rugged, and the soil is loose and fragile, consisting of clay and marble.

# 3.3. Soil erosion rates about precipitation, erosivity, and factor C for the period 1999–2040

Climate change can lead to changes in precipitation patterns, both in terms of annual values and seasonal distribution (Sohoulande Djebou and Singh, 2016), which can significantly modify the erosivity factors (R) and vegetation cover (C) and, thus, soil loss rates. To protect the soil from water erosion caused by the impact of climate change and to take necessary measures to guide anthropogenic activities in the Loukkos watershed, such as agricultural practices, we reconstructed the spatio-

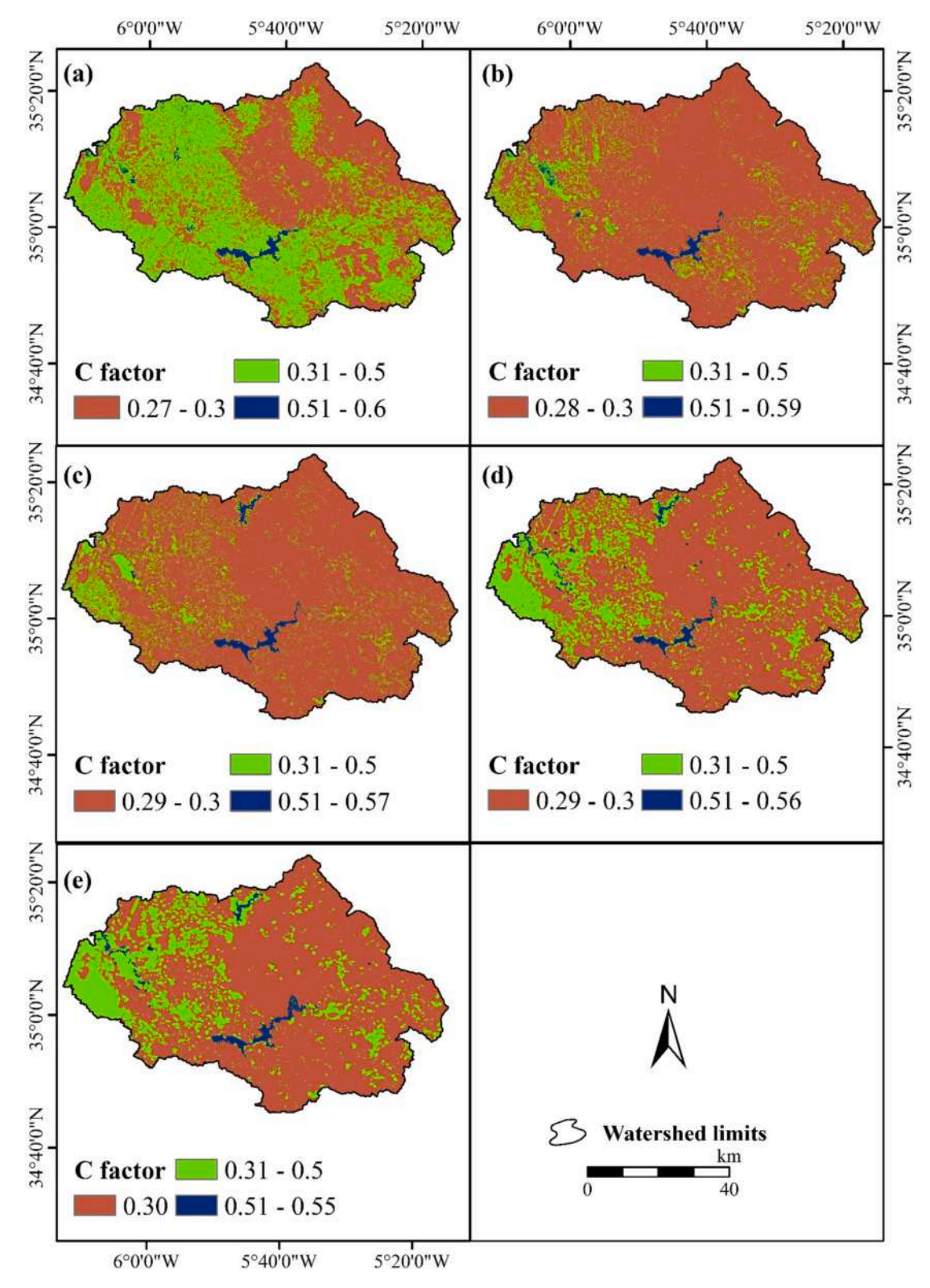


Fig. 7. Spatial distribution of the C-Factor for Loukkos watershed. (a) 1999, (b) 2009, (c) 2019, (d) 2029, and (e) 2040.

temporal evolution of precipitation and NDVI for 1999–2040. We identified the expected scenarios of changes in vegetation cover, erosivity, and soil loss while deducing the degree of correlation between them. On the one hand, the analyses demonstrate that a change in precipitation will inevitably lead to a change in NDVI values, thereby affecting the estimation of the C factor for an accurate soil loss prediction. While precipitation is positively correlated with NDVI with a value

of  $R^2=0.76$  (Fig. 9a) and negatively correlated with the C factor with a value of  $R^2=0.77$  (Fig. 9b), indicating that a positive change in precipitation will result in a positive change in NDVI and an adverse change in the C factor.

On the other hand, the results revealed that precipitation also affects erodibility and soil loss, which are closely related (Fig. 9c). Fig. 9d confirms a strong positive correlation between erodibility and soil loss,

**Table 6**Distribution of the C-factor classes over the Loukkos watershed.

		1999	2009	2019	2029	2040
Class	Values	Area (%)	Area (%)	Area (%)	Area (%)	Area (%)
Low Moderate High	<0.3 0.31–0.5 ≥0.51	49.61 48.95 1.44	86.63 11.96 1.41	86.94 11.64 1.43	75.73 22.51 1.76	75.82 22.23 1.95

as the  ${\rm R}^2$  value is 0.99. This indicates that when annual erodibility increases, soil loss values increase, and vice versa, provided other conditions remain the same.

Based on these results, we conclude that precipitation is the dominant factor affecting erodibility, vegetation dynamics, and soil loss. The significant changes between 1999 and 2040 indicate that factor C decreased from the highest value of 0.36 in 1999 to the lowest value of 0.30 in 2009 (Fig. 9b), demonstrating that this factor is not the main cause of increased soil loss in the basin. By examining Figs. 3 and 8, we find that soil loss primarily occurs in areas with the highest erodibility values, indicating that the latter remains the primary determinant of soil loss in the Loukkos watershed (Fig. 9c and d).

#### 3.4. Validation

#### 3.4.1. Sediment yield and silting rate of the Oued El Makhazine dam

We utilized the sediment delivery ratio (SDR) model to determine the proportion of eroded soils due to water erosion that contributes to sedimentation in the reservoir area of the watershed (Wu et al., 2018), which is best suited for the area. Consequently, the coupled RUSLE/SDR model was employed to calculate sediment yield (SY) by Ouadjane et al. (2021). From these data, we obtained a sediment delivery ratio (SDR) of 21.2 % (Table 8) and a sediment yield (SY) value of 8,849,672.16  $t.ha^{-1}.year^{-1}$ , corresponding to 6.81 Mm<sup>3</sup> (Table 9), which matches the value measured by the bathymetry conducted by the Loukkos Hydraulic Basin Agency (ABHL) at the El Makhazine dam reservoir (Table 10).

#### 4. Discussion

To clarify and evaluate the results obtained in this article, we compared them to a set of studies aimed at determining soil loss rates due to water erosion in different regions of Morocco. Consequently, we found significant spatial differences between the obtained soil loss values, in the Ourika watershed in the High Atlas of Marrakech. Meliho et al. (2016) found an average soil loss value of 380  $t.ha^{-1}$ . year<sup>-1</sup>, with  $48\,\%$  of the watershed area experiencing soil loss ranging from 50 to  $400\,$ t.ha<sup>-1</sup>.year<sup>-1</sup>, 30 % between 400 and 1000 t.ha<sup>-1</sup>.year<sup>-1</sup>, and only 4 % below the tolerance threshold ( $<7t.ha^{-1}.year^{-1}$ ). Meanwhile, in the Oum Er-Rbia watershed in the Middle Atlas, El Jazouli et al. (2019) showed that the average soil loss was 250 t.ha<sup>-1</sup>.year<sup>-1</sup>.A study by Ouadjane et al. (2021) found that 22.5 % of the area is very vulnerable to erosion. He was also conducted in the Agoudal watershed in the Central High Atlas, southeast of Morocco. He found an average erosion value of 255.058 t.ha<sup>-1</sup>.year<sup>-1</sup> using the RUSLE model. In contrast, in northern Morocco, on the Mediterranean slope of the western Rif, in the Oued Arbaa Ayacha watershed. Ouallali et al. (2016) found that the estimated annual soil loss varied between 0.11 and 468  $t.ha^{-1}.year^{-1}$ , while in the Oued Tleta watershed, Zahnoun and Jamal (2020) reported that the maximum soil loss value was about 294  $t.ha^{-1}.year^{-1}$ , with an average loss estimated at 46.1 t.ha<sup>-1</sup>.year<sup>-1</sup> and a total annual loss of about 800,000  $t.ha^{-1}.year^{-1}$ .

Further research conducted in the Rif region reveals a higher level of erosion risk in this watershed, with soil loss rates ranging from 0 to  $467.19 \ t.ha^{-1}.year^{-1}$ , 0 to  $3797.66 \ t.ha^{-1}.year^{-1}$ , 0 to 1810.83

 $t.ha^{-1}.year^{-1}$ , 0 to 631.72  $t.ha^{-1}.year^{-1}$ , and 0 to 932.53  $t.ha^{-1}.year^{-1}$  in 1999, 2009, 2019, 2029, and 2040, respectively. Compared to findings in other watersheds, such as Arbaa Ayacha (Ouallali et al., 2016) with soil loss between 0.11 and 468  $t.ha^{-1}.year^{-1}$ , Tahaddart (Tahiri et al., 2017) where values ranged from 0 to 202.3  $t.ha^{-1}.year^{-1}$ .

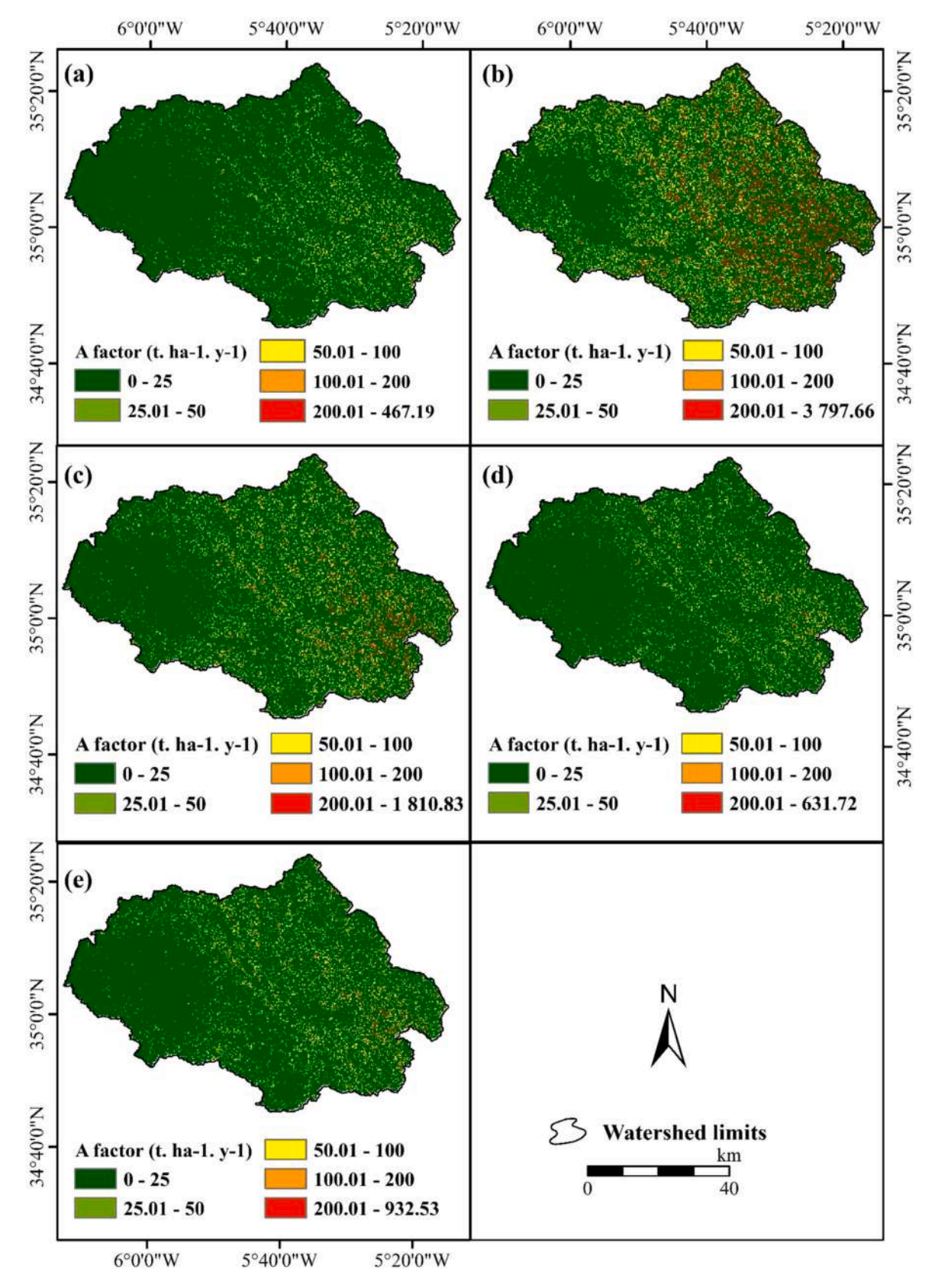
However, further research conducted in the Rif region supports our findings, particularly in the El Kharroub watershed (Ammari et al., 2023; F. Li et al., 2024). Estimated annual erosion rates range from 0.47 to 1284.7  $t.ha^{-1}.year^{-1}$  between 2000 and 2020, from 0.37 to 1007.6  $t.ha^{-1}.year^{-1}$  for the period 2021–2030, and from 0.36 to 1012.6  $t.ha^{-1}.year^{-1}$  for 2031–2050. In the Oued El Makhazine watershed (a sub-basin of Loukkos), Bassairate et al. (2021) reported an average annual soil loss of approximately 101.2  $t.ha^{-1}.year^{-1}$  between 1999 and 2008, and 174.5  $t.ha^{-1}.year^{-1}$  between 2008 and 2013. These figures highlight the severity of the erosion issue in the region and the need for immediate action to address it (Xiong et al., 2024).

Compare the results of various studies conducted across the Mediterranean basin to evaluate the accuracy of the model used. For example, according to a study by Kaci et al. (2017), average soil losses on fragile lands in the Oued Rhiou basin in Algeria reach  $25\ t.ha^{-1}.year^{-1}$ . Similarly, (Souadi, 2011) reports that the Oued Barbara basin in Tunisia loses an average of  $36\ t.ha^{-1}.year^{-1}$ . Focusing on the Mhaydssé watershed in the Bekaa plain of Lebanon, (El Hage et al., 2016) estimate soil losses at  $46\ t.ha^{-1}.year^{-1}$ . On the other side of the Mediterranean, a study by Napoli et al. (2016) in the Tusciano river basin in Italy reports average losses of  $22\ t.ha^{-1}.year^{-1}$  using the RUSLE model. In Spain, researchers such as García-Ruiz (2010) observed high erosion rates ranging from  $30.2\ to\ 80.4\ t.ha^{-1}.year^{-1}$  in various sub-basins of the Segura river. These figures underscore the importance of considering regional differences to better understand and manage soil erosion in the Mediterranean region (Liu et al., 2024; Qi et al., 2023).

The study highlights the extent of annual soil loss in the Loukkos basin between 1999 and 2040, revealing an alarming situation. This deterioration is primarily attributed to changes in erosion intensity caused mainly by climatic variations (precipitation), as confirmed by this research and previous studies, including those by Napoli et al. (2016) in Ethiopia, Zahnoun and Jamal (2020) in China, Ouadjane et al. (2021) in Iran, Meliho et al. (2016) in Spain, and Ammari et al. (2023) in Thailand. However, it is important to note that other factors significantly contribute to the uneven distribution of soil erosion risks, adding further complexity to this urgent environmental issue.

In this regard, it is strongly recommended to implement on-site soil conservation practices. For example, a study by Gong et al. (2022) demonstrated that mixed forests significantly reduced soil erosion by 23.6 % compared to monocultures. Moreover, the results showed that this effectiveness was particularly notable on steep slopes, between 16 and 25°. However, farmers should also consider other soil conservation measures on their agricultural lands. For instance, early crop sowing is preferable to late sowing. A study by Meunier et al. (2011) demonstrated that early planting of cassava helps mitigate soil erosion by promoting vegetation cover development and reducing runoff. Additionally, constructing terraces on steep terrain has proven to be an effective method for slowing runoff velocity, as highlighted by Chen et al. (2017).

This study, while providing valuable insights into soil erosion dynamics and sediment yield forecasting in the Loukkos watershed, faces several data limitations that may influence the precision of its results. The accuracy of the RUSLE and SDR models heavily depends on the quality and resolution of input data such as precipitation, LULC, and soil properties. The future precipitation projections were derived from a LME model based on historical data from 1999 to 2019, which may not fully capture the complexity of future climate patterns, especially in the face of extreme weather events. Similarly, the NDVI predictions using the CA-Markov model are constrained by the resolution and frequency of available satellite imagery, which may not reflect rapid changes in



 $\textbf{Fig. 8.} \ \ \textbf{Spatial distribution of estimated soil erosion rates in the study area: (a) 1999, (b) 2009, (c) 2019, (d) 2029, and (e) 2040.$ 

**Table 7**Classes of soil loss rates derived from the RUSLE model.

		1999		2009		2019		2029		2040	
Values t.ha <sup>-1</sup> .year <sup>-1</sup>	Class	%	km <sup>2</sup>	%	km <sup>2</sup>	%	km <sup>2</sup>	%	km <sup>2</sup>	%	km <sup>2</sup>
<25	Low	92.21	3451.9	78.24	2928.8	85.55	3202.44	90.99	3406.02	88.88	3327.34
25-50	Moderate	4.43	165.83	5.5	206.06	6.08	227.55	4.99	186.7	5.59	209.3
50-100	High	2.43	91.08	5.94	222.39	4.47	167.27	2.81	105.06	3.58	134.14
100-200	Very High	0.8	30.04	4.97	186.01	2.56	95.83	1.04	39.06	1.55	58.01
>200	Extremely High	0.12	4.62	5.35	200.2	1.35	50.36	0.18	6.61	0.39	14.67
Total	-	100	3743.46	100	3743.46	100	3743.46	100	3743.46	100	3743.46
Min	_	0		0		0		0		0	
Max	_	467.19		3797.66		1810.83		631.72		932.53	
Average	_	100.64		138.27		110.98		103.5		104.16	

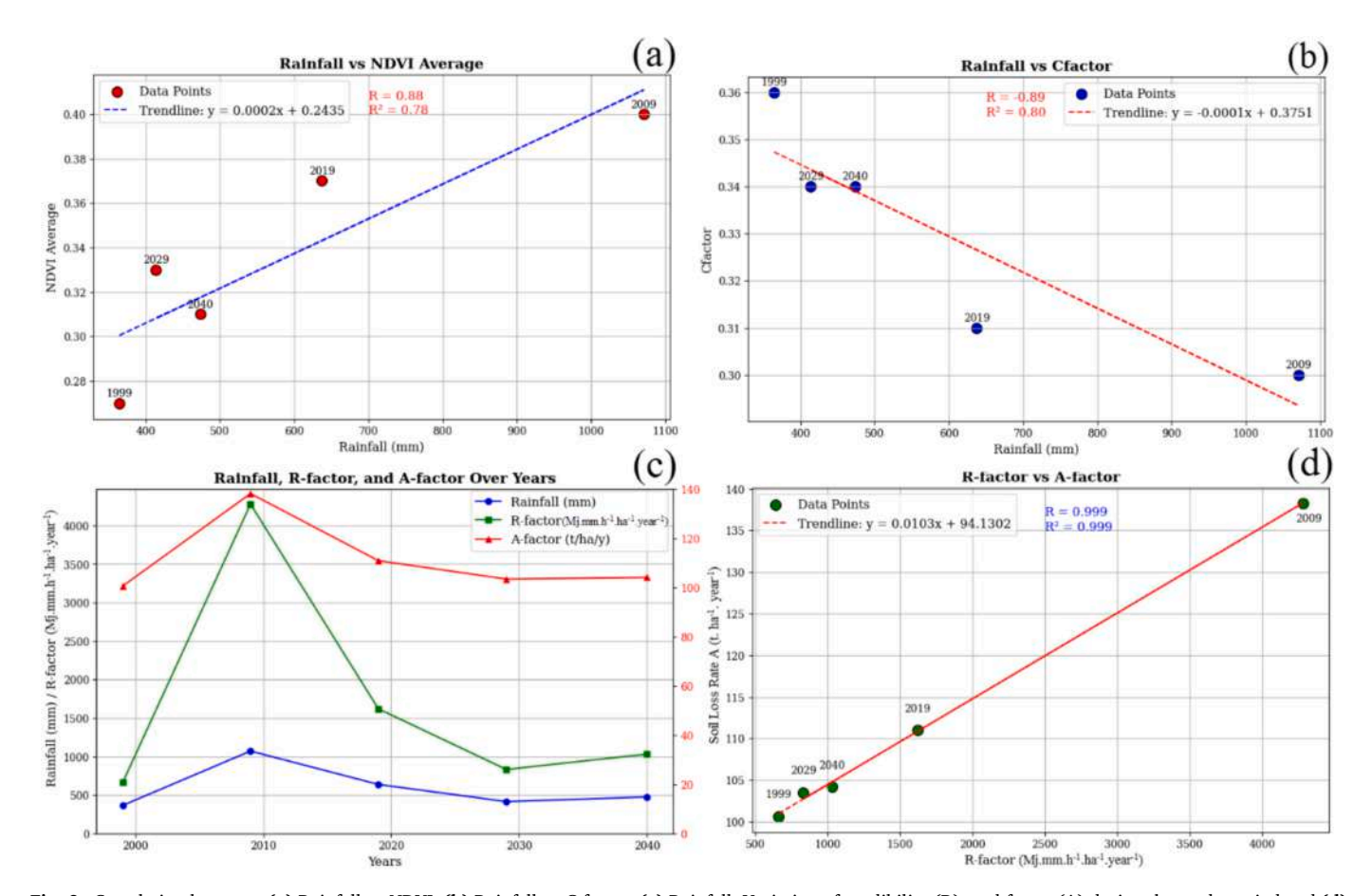


Fig. 9. Correlation between: (a) Rainfall vs NDVI, (b) Rainfall vs C-factor, (c) Rainfall, Variation of erodibility (R), and factor (A) during the study period and (d) Correlation between R-factor vs A-factor.

**Table 8**Estimation of SDR.

Model name	Model equation	A (km <sup>2</sup> )	SDR
Zhao and Shi (2002)	$SDR=0.735^*\big(A^{-0.151}\big)$	3743.46	0.212189108

**N.B.:** The bulk density of the area is estimated at 1300 kg/m<sup>3</sup>.

vegetation cover caused by unforeseen human activities or climatic fluctuations. Additionally, the sediment yield validation is based on data from the El Makhazine dam reservoir, which, although useful, may not comprehensively represent sediment dynamics across the entire watershed. Despite these limitations, the study employs robust statistical methods and validation techniques, ensuring that its findings remain reliable within the constraints of available data.

This research contributes directly to several Sustainable Development Goals (SDGs), particularly SDG 13 (Climate Action), SDG 15 (Life

**Table 9**The sediment yield estimated by RUSLE/SDR for the Loukkos watershed for the period 1999–2040.

Name	Area (A) ha <sup>-1</sup>	Mean loss t.ha <sup>-1</sup> .year <sup>-1</sup>	Erosion rate $t.year^{-1}$	SY	SY (t.year <sup>-1</sup> r)	SY (Mm <sup>3</sup> )
Joukkos Basin	374,345.84	111.51	41,743,736.61	$SY = SDR \times A$	8,849,672.16	6.81

Table 10
Bathymetric measurements of the Oued el Makhazine Dam (Loukkos).

Year	1979–1985	1985–1990	1990–2001	2001–2002	2002–2008	2008-2013
Normal Volume (Mm³) Volume Difference (Mm³) Annual Loss (Mm³) Mean Annual Loss (Mm³)	807.00 6.05 1.01 6.81	800.95 28.24 5.65	772.72 48.83 4.44	723.89 24.50 24.50	699.39 0.43 0.07	698.96 26.10 5.22

on Land), and SDG 6 (Clean Water and Sanitation). By forecasting soil erosion and sediment yield under changing climatic conditions, the study offers crucial information for climate adaptation strategies, helping policymakers take proactive measures to mitigate land degradation and preserve soil health (SDG 15). The identification of priority areas for erosion control supports ecosystem protection, ensuring sustainable land management and combating desertification. Furthermore, the findings are critical for maintaining water quality in reservoirs and rivers by reducing sedimentation, which aligns with SDG 6 by promoting better water resource management. Ultimately, this study exemplifies how integrated geospatial techniques and predictive models can aid in achieving long-term environmental sustainability, resilience, and improved natural resource management in vulnerable regions.

#### 5. Conclusions

This study introduces a method to forecast and estimate the average annual soil loss rate and average sediment yield (SY) in the Loukkos watershed in Morocco for the period 1999–2040, aiming to assess climate change impacts on soil degradation. The approach combines the RUSLE/SDR model with forecasting models. Future precipitation projections until 2040 were simulated using a LME based on daily precipitation data from 1999 to 2019. Additionally, the CA-Markov model predicted the NDVI for 2029 and 2040 based on 1999, 2009, and 2019 data. The accuracy of the precipitation forecast simulation was confirmed by a "p-value" <0.05 and low standard deviation values for both fixed and random effects, aligning well with adjusted values. NDVI forecast simulation was validated by kappa index values indicating strong consistency between simulated and actual NDVI maps.

The results showed erosion rates in the Loukkos basin varied from 0 to  $3797.66 \, t.ha^{-1}.year^{-1}$  with an SDR of  $21.2 \, \%$  and an average loss of  $111.51 \, t.ha^{-1}.year^{-1}$ . The highest average soil loss was in 2009, and the lowest was in 1999. Soil loss significantly increased by  $37.39 \, \%$  from 1999 to 2009, then decreased by  $19.74 \, \%$  from 2009 to 2019, and is expected to decrease by  $6.75 \, \%$  from 2019 to 2029, with a slight increase of  $0.64 \, \%$  from 2029 to 2040. A strong positive correlation exists between erosivity and soil loss ( $R^2 = 0.99$ ). Precipitation changes primarily affect the soil cover factor (C) and erosivity (R), leading to soil loss mainly in the eastern region of the basin, characterized by fragile soils, rugged terrain, and lack of vegetation. Erosivity remains the main determinant of soil loss in the Loukkos watershed. The sediment yield estimated by RUSLE/SDR matches the measured value at the El Makhazine dam reservoir.

The study demonstrates that prediction models effectively simulate and forecast scenarios of the adopted factors. Integrating the RUSLE-SDR model with remote sensing and GIS for estimating soil loss and sediment yield provides a flexible spatial analysis and data processing environment, assisting decision-makers in assessing soil losses and identifying priority areas for erosion protection and control at a low cost.

## CRediT authorship contribution statement

**Belhaj Fatima:** Writing – review & editing, Writing – original draft, Validation, Software, Data curation, Conceptualization. **Hlila Rachid:** Writing – review & editing, Writing – original draft, Supervision, Software, Resources. **Belkendil Abdeldjalil:** Writing – review & editing,

Writing – original draft, Validation, Project administration, Investigation. **Ouallali Abdessalam:** Writing – review & editing, Writing – original draft, Software, Methodology. **Beroho Mohamed:** Writing – review & editing, Writing – original draft, Software, Resources, Funding acquisition, Formal analysis, Data curation. **Alanoud T. Alfagham:** Writing – original draft, Writing – review & editing. **Aqil Tariq:** Writing – review & editing, Writing – original draft, Software, Resources, Supervision, Validation, Visualization.

#### **Funding**

The authors extend their appreciation to the Researchers supporting project number (RSPD2025R558) King Saud University, Riyadh, Saudi Arabia.

#### Declaration of competing interest

The authors declare that they have no known competing financial interests or personal relationships that could have appeared to influence the work reported in this paper.

## Acknowledgements

The authors extend their appreciation to the Researchers supporting project number (RSPD2025R558) King Saud University, Riyadh, Saudi Arabia.

## Appendix A. Supplementary data

Supplementary data to this article can be found online at https://doi.org/10.1016/j.apsoil.2025.105910.

#### Data availability

Data will be made available on request.

#### References

Abbou, M., Chabbi, M., Benicha, M., 2023. Assessment of phytosanitary practices on the environment: case study potato of Loukkos (Northwest Morocco). Environ. Monit. Assess. 195. https://doi.org/10.1007/s10661-023-10949-9.

Abdelkarim, A., 2023. Monitoring and forecasting of land use/land cover (LULC) in Al-Hassa oasis, Saudi Arabia based on the integration of the cellular automata (CA) and the cellular automata-Markov model (CA-Markov). Geol. Ecol. Landscapes 00, 1–32. https://doi.org/10.1080/24749508.2022.2163741.

Abdelwahab, O.M.M., Ricci, G.F., De Girolamo, A.M., Gentile, F., 2018. Modelling soil erosion in a Mediterranean watershed: comparison between SWAT and AnnAGNPS models. Environ. Res. 166, 363–376. https://doi.org/10.1016/j.envres.2018.06.029.

Acharki, S., Taia, S., Arjdal, Y., Hack, J., 2023. Hydrological modeling of spatial and temporal variations in streamflow due to multiple climate change scenarios in northwestern Morocco. Clim. Serv. 30, 100388. https://doi.org/10.1016/j. cliser.2023.100388.

Ahmed, M., Aqnouy, M., Stitou El Messari, J., 2021. Sustainability of Morocco's groundwater resources in response to natural and anthropogenic forces. J. Hydrol. 603. https://doi.org/10.1016/j.jhydrol.2021.126866.

Alitane, A., Essahlaoui, A., El Hafyani, M., El Hmaidi, A., El Ouali, A., Kassou, A., El Yousfi, Y., van Griensven, A., Chawanda, C.J., Van Rompaey, A., 2022. Water Erosion monitoring and prediction in response to the effects of climate change using RUSLE and SWAT equations: case of R'Dom watershed in Morocco. Land 11. https://doi.org/10.3390/land11010093.

Almouctar, M.A.S., Wu, Y., Zhao, F., Dossou, J.F., 2021. Soil erosion assessment using the rusle model and geospatial techniques (remote sensing and gis) in south-Central

- Niger (Maradi region). Water (Switzerland) 13. https://doi.org/10.3390/wil3243511
- Ammari, Z., Mili, E.M., Essahlaoui, A., El Hafyani, M., Essahlaoui, N., Boufala, M., Ouallali, A., Berrad, F., Aassoumi, H., 2023. Mapping and predicting of water Erosion using Rusle in the Mediterranean context: case of El Kharroub watershed (Western Rif, northern Morocco). ARPN J. Eng. Appl. Sci. 18, 651–661. https://doi.org/10.59018/032391.
- Bammou, Y., Benzougagh, B., Bensaid, A., Igmoullan, B., Al-Quraishi, A.M.F., 2024.
  Mapping of current and future soil erosion risk in a semi-arid context (haouz plain Marrakech) based on CMIP6 climate models, the analytical hierarchy process (AHP) and RUSLE. Model. Earth Syst. Environ. 10, 1501–1514. https://doi.org/10.1007/s40808-023-01845-9.
- Bassairate, O., Chikhaoui, M., Naimi, M., Sabir, M., 2021. Effets de la dynamique de la végétation sur le rythme d'envasement et la disponibilité de l'eau dans le barrage Makhazine (Maroc). Rev. Mar. Sci. Agron. Vét 9, 553–561.
- Belhaj, F., Hlila, R., El Kadiri, K., Ouallali, A., Belkendil, A., Beroho, M., Aqil, T., Davis Brian, J., Walid, S., 2024. Modelling, quantification and estimation of the soil water erosion using the revised universal soil loss equation with sediment delivery ratio and the analytic hierarchy process models. Earth Surf. Process. Landf. 1–19. https:// doi.org/10.1002/esp.5882.
- Belkendil, A., Haddad, S., Hamouine, A., Habi, M., 2016. Contribution to the solid transport study of the lower Guir watershed. South-West of Algeria 7.
- Beroho, M., Briak, H., El Halimi, R., Ouallali, A., Boulahfa, I., Mrabet, R., Kebede, F., Aboumaria, K., 2020. Analysis and prediction of climate forecasts in northern Morocco: application of multilevel linear mixed effects models using R software. Heliyon 6, e05094. https://doi.org/10.1016/j.heliyon.2020.e05094.
- Bezak, N., Borrelli, P., Mikoš, M., Jemec Auflič, M., Panagos, P., 2024. Towards multi-model soil erosion modelling: an evaluation of the erosion potential method (EPM) for global soil erosion assessments. Catena 234. https://doi.org/10.1016/j.catena.2023.107596.
- Bijay-, Singh, Craswell, E., 2021. Fertilizers and nitrate pollution of surface and ground water: an increasingly pervasive global problem. SN Appl. Sci. 3, 1–24. https://doi. org/10.1007/s42452-021-04521-8.
- Borrelli, P., Robinson, D.A., Panagos, P., Lugato, E., Yang, J.E., Alewell, C., Wuepper, D., Montanarella, L., Ballabio, C., 2020. Land use and climate change impacts on global soil erosion by water (2015-2070). Proc. Natl. Acad. Sci. USA 117, 21994–22001. https://doi.org/10.1073/pnas.2001403117.
- Boufeldja, S., Baba Hamed, K., Bouanani, A., Belkendil, A., 2020. Identification of zones at risk of erosion by the combination of a digital model and the method of multicriteria analysis in the arid regions: case of the Bechar Wadi watershed. Appl Water Sci 10. https://doi.org/10.1007/s13201-020-01191-6.
- Chalise, D., Kumar, L., Kristiansen, P., 2019. Land degradation by soil erosion in Nepal: a review. Soil Syst. https://doi.org/10.3390/soilsystems3010012.
- Chen, D., Wei, W., Chen, L., 2017. Effects of terracing practices on water erosion control in China: a meta-analysis. Earth-Science Rev. 173, 109–121. https://doi.org/ 10.1016/j.earscirev.2017.08.007.
- Chen, L., Wang, Q., Zhu, G., Lin, X., Qiu, D., Jiao, Y., Lu, S., Li, R., Meng, G., Wang, Y., 2024. Dataset of stable isotopes of precipitation in the Eurasian continent. Earth Syst. Sci. Data 16, 1543–1557. https://doi.org/10.5194/essd-16-1543-2024.
- Chuenchum, P., Xu, M., Tang, W., 2020. Estimation of soil erosion and sediment yield in the lancang-mekong river using the modified revised universal soil loss equation and GIS techniques. Water (Switzerland) 12. https://doi.org/10.3390/w12010135.
- Cui, L., Zhao, Y., Liu, J., Wang, H., Han, L., Li, J., Sun, Z., 2021. Vegetation coverage prediction for the qinling mountains using the ca–markov model. ISPRS Int. J. Geo-Information 10. https://doi.org/10.3390/ijgi10100679.
- Cui, Z., Chen, Q., Luo, J., Ma, X., Liu, G., 2024. Characterizing subsurface structures from hard and soft data with multiple-condition fusion neural network. Water Resour. Res. 60, e2024WR038170, https://doi.org/10.1029/2024WR038170
- Res. 60, e2024WR038170. https://doi.org/10.1029/2024WR038170.

  Daliakopoulos, I.N., Panagea, I.S., Tsanis, I.K., Grillakis, M.G., Koutroulis, A.G.,

  Hessel, R., Mayor, A.G., Ritsema, C.J., 2017. Yield response of Mediterranean
  rangelands under a changing climate. L. Degrad. Dev. 28, 1962–1972. https://doi.
  org/10.1002/dr.2717.
- De Chazal, J., Rounsevell, M.D.A., 2009. Land-use and climate change within assessments of biodiversity change: a review. Glob. Environ. Chang. 19, 306–315. https://doi.org/10.1016/j.gloenvcha.2008.09.007.
- Derpsch, R., Kassam, A., Reicosky, D., Friedrich, T., Calegari, A., Basch, G., Gonzalez-Sanchez, E., dos Santos, D.R., 2024. Nature's laws of declining soil productivity and conservation agriculture. Soil Secur. 14, 100127. https://doi.org/10.1016/j.soisec.2024.100127
- Dos Santos, J.C.N., De Andrade, E.M., Medeiros, P.H.A., Palácio, H.A. de Q., Neto, J.R. de A., 2017. Sediment delivery ratio in a small semi-arid watershed under conditions of low connectivity. Rev. Ciênc. Agron. 48, 49–58. doi:https://doi.org/10.5935/180
- Du, C., Bai, X., Li, Y., Tan, Q., Zhao, C., Luo, G., Wang, J., Wu, L., Li, C., Li, J., Xie, Y., Ran, C., Zhang, S., Xiong, L., Yuang, X., Liao, J., Dai, L., Long, M., Li, Z., Xue, Y., Zhang, X., Luo, Q., Shen, X., Yang, S., Li, M., 2024. The restoration of karst rocky desertification has enhanced the carbon sequestration capacity of the ecosystem in southern China. Glob. Planet. Change 243, 104602. https://doi.org/10.1016/j.gloplacha.2024.104602.
- Durigon, V.L., Carvalho, D.F., Antunes, M.A.H., Oliveira, P.T.S., Fernandes, M.M., 2014. NDVI time series for monitoring RUSLE cover management factor in a tropical watershed. Int. J. Remote Sens. 35, 441–453. https://doi.org/10.1080/ 01431161.2013.871081.
- Eekhout, J.P.C., De Vente, J., 2020. How soil erosion model conceptualization affects soil loss projections under climate change. Prog. Phys. Geogr. 44, 212–232. https://doi. org/10.1177/0309133319871937.

- Assaoui, N. El, Bouiss, C.E., Sadok, A., 2023. Assessment of water Erosion by integrating RUSLE model, GIS and remote sensing case of Tamdrost watershed (Morocco). Ecol. Eng. Environ. Technol. 24, 43–53. https://doi.org/10.12912/27197050/
- El Hage, H., Touchart, L., Ardillier-carras, F., Faour, G., 2016. Lutte contre l'érosion et aménagement agricole dans la plaine de la Bekaa (Liban). M@ppemonde 117.
- El Jazouli, A., Barakat, A., Khellouk, R., 2019a. GIS-multicriteria evaluation using AHP for landslide susceptibility mapping in Oum Er Rbia high basin (Morocco). Geoenviron. Disasters 6. https://doi.org/10.1186/s40677-019-0119-7.
- Jazouli, A. El, Barakat, A., Khellouk, R., Rais, J., Baghdadi, M. El, 2019b. Remote sensing and GIS techniques for prediction of land use land cover change effects on soil erosion in the high basin of the Oum Er Rbia River (Morocco). Remote Sens. Appl. Soc. Environ. 13, 361–374. https://doi.org/10.1016/j.rsase.2018.12.004.
- Eniyew, S., Teshome, M., Sisay, E., Bezabih, T., 2021. Integrating RUSLE model with remote sensing and GIS for evaluation soil erosion in Telkwonz watershed, northwestern Ethiopia. Remote Sens. Appl. Soc. Environ. 24, 100623. https://doi. org/10.1016/j.rsase.2021.100623.
- García-Ruiz, J.M., 2010. The effects of land uses on soil erosion in Spain: a review. Catena 81, 1–11. https://doi.org/10.1016/j.catena.2010.01.001.
- Getachew, B., Manjunatha, B.R., Bhat, G.H., 2021. Assessing current and projected soil loss under changing land use and climate using RUSLE with remote sensing and GIS in the Lake Tana Basin, upper Blue Nile River basin, Ethiopia. Egypt. J. Remote Sens. Sp. Sci. 24, 907–918. https://doi.org/10.1016/j.ejrs.2021.10.001.
- Girmay, G., Moges, A., Muluneh, A., 2021. Assessment of current and future climate change impact on soil loss rate of Agewmariam watershed, northern Ethiopia. Air, Soil Water Res. 14. https://doi.org/10.1177/1178622121995847.
- Gong, C., Tan, Q., Liu, G., Xu, M., 2022. Impacts of mixed forests on controlling soil erosion in China. Catena 213, 106147. https://doi.org/10.1016/j. catena 2022 106147
- Hrour, Y., Fovet, O., Lacombe, G., Rousseau-Gueutin, P., Sebari, K., Pichelin, P., Thomas, Z., 2023. A framework to assess future water-resource under climate change in northern Morocco using hydro-climatic modelling and water-withdrawal scenarios. J. Hydrol. Reg. Stud. 48. https://doi.org/10.1016/j.ejrh.2023.101465.
- Jie, C., Jing-zhang, C., Man-zhi, T., Zi-tong, G., 2002. Soil degradation: a global problem endangering sustainable development. J. Geogr. Sci. 12, 243–252. https://doi.org/ 10.1007/bf02837480.
- Jin, F., Yang, W., Fu, J., Li, Z., 2021. Effects of vegetation and climate on the changes of soil erosion in the loess plateau of China. Sci. Total Environ. 773, 145514. https:// doi.org/10.1016/j.scitotenv.2021.145514.
- Kaci, M., Habi, M., Morsli, B., 2017. Estimation de l'érosion hydrique par l'application de l'équation universelle de pertes en sol (USLE). Cas du bassin versant non jaugé de l'oued Rhiou, (Bassin de Cheliff) Algérie. Geo. Eco. Trop. 41, 503–518.
- Kidane, D., Bahir, A., Yosef, B.A., 2015. The effect of upstream land use practices on soil
   Erosion and sedimentation in the upper Blue Nile Basin, Ethiopia BDU-IUC project 3
   water management and its implications to the hydro-system dynamics in the Tana-Beles area, upper Blue Nile basin view pr. Res. J. Agric. Environ. Manag. 4, 055–068.
- Kosmas, C., Danalatos, N.G., Gerontidis, S., 2000. The effect of land parameters on vegetation performance and degree of erosion under Mediterranean conditions. Catena 40, 3–17. https://doi.org/10.1016/S0341-8162(99)00061-2.
- Lee, M.H., Lin, H.H., 2015. Evaluation of annual rainfall erosivity index based on daily, monthly, and annual precipitation data of rainfall station network in southern Taiwan. Int. J. Distrib. Sens. Networks 2015. https://doi.org/10.1155/2015/214708
- Li, F., Shan, Y., Li, M., Guo, Y., Liu, C., 2024. Insights for river restoration: the impacts of vegetation canopy length and canopy discontinuity on riverbed evolution. Water Resour. Res. 60, e2023WR036473. https://doi.org/10.1029/2023WR036473.
- Li, J., Xiong, M., Sun, R., Chen, L., 2024. Temporal variability of global potential water erosion based on an improved USLE model. Int. Soil Water Conserv. Res. 12, 1–12. https://doi.org/10.1016/j.iswcr.2023.03.005.
- Liou, Y.A., Nguyen, Q.V., Hoang, D.V., Tran, D.P., 2022. Prediction of soil erosion and sediment transport in a mountainous basin of Taiwan. Prog Earth Planet Sci 9. https://doi.org/10.1186/s40645-022-00512-4.
- Liu, Z., Qiu, H., Zhu, Y., Huangfu, W., Ye, B., Wei, Y., Tang, B., Kamp, U., 2024. Increasing irrigation-triggered landslide activity caused by intensive farming in deserts on three continents. Int. J. Appl. Earth Obs. Geoinf. 134, 104242. https://doi. org/10.1016/j.jag.2024.104242.
- Meliho, M., Abdellatif, K., Nadia, M., Zhang, H., 2016. Cartographie des Risques De L'erosion Hydrique par L'equation Universelle Revisee des Pertes En sols, La Teledetection et les sig Dans Le Bassin versant De L'ourika (haut atlas, Maroc). Eur. Sci. Journal, ESJ 12, 277. https://doi.org/10.19044/esj.2016.v12n32p277.
- Meunier, Q., Lassois, L., Doucet, J., 2011. DACEFI-2: Développement d'Alternatives Communautaires à l'Exploitation Forestière Illégale (seconde phase) Guide de plantation et de conduite d'une bananeraie agroforestière en milieu rural au Gabon. Proj. DACEFI-2 sous Financ. l'Union Eur. 32.
- Napoli, M., Cecchi, S., Orlandini, S., Mugnai, G., Zanchi, C.A., 2016. Simulation of field-measured soil loss in Mediterranean hilly areas (chianti, Italy) with RUSLE. Catena 145, 246–256. https://doi.org/10.1016/j.catena.2016.06.018.
- Nie, L.C., Liu, Z.M., Liu, Y.X., 2015. Linear and segmented linear trend vegetation index data in semiarid GIMMS normalized difference detection for vegetation cover using regions of Nigeria. J. Appl. Remote. Sens. 9, 551–556. https://doi.org/10.1117/1. IDS 0
- Ochoa, P.A., Fries, A., Mejía, D., Burneo, J.I., Ruíz-Sinoga, J.D., Cerdà, A., 2016. Effects of climate, land cover and topography on soil erosion risk in a semiarid basin of the Andes. Catena 140, 31–42. https://doi.org/10.1016/j.catena.2016.01.011.
- Ouadjane, Y., Ait Yacine, E.-A., Benzougagh, B., Nassiri, L., Ibijbijen, J., 2021. Evaluation Des Risques D'érosion Hydrique Et Cartographie Des Zones Vulnérables Par La

- Méthode RUSLE Couplée Aux SIG Et À La Télédétection Dans Le Bassin Versant d'Agoudal En Amont De La Vallée d'Imilchil (Haut Atlas Central, Maroc). European Scientific Journal, ESJ. 66. https://doi.org/10.19044/esj.2021.v17n21p66.
- Ouallali, A., Moukhchane, M., Aassoumi, H., Berrad, Dakir, I., 2016. Evaluation et carto graphie des taux d'érosion hydrique dans le bassin versant de l'Oued Arbaa Ayacha (Rif occidental, Nord Maroc) Evaluation and mapping of water erosion rates in the watershed of the Arbaa Ayacha River (Western Rif, Northern Mor. (Bull. l'Institut Sci. Rabat, Sect. Sci. la Terre 65–79).
- Panagos, P., Borrelli, P., Meusburger, K., van der Zanden, E.H., Poesen, J., Alewell, C., 2015. Modelling the effect of support practices (P-factor) on the reduction of soil erosion by water at European scale. Environ. Sci. Pol. 51, 23–34. https://doi.org/ 10.1016/i.envsci.2015.03.012.
- Panagos, P., Ballabio, C., Himics, M., Scarpa, S., Matthews, F., Bogonos, M., Poesen, J., Borrelli, P., 2021. Projections of soil loss by water erosion in Europe by 2050. Environ. Sci. Pol. 124, 380–392. https://doi.org/10.1016/j.envsci.2021.07.012.
- Paroissien, J.B., Darboux, F., Couturier, A., Devillers, B., Mouillot, F., Raclot, D., Le Bissonnais, Y., 2015. A method for modeling the effects of climate and land use changes on erosion and sustainability of soil in a Mediterranean watershed (Languedoc, France). J. Environ. Manag. 150, 57–68. https://doi.org/10.1016/j. jenyman.2014.10.034.
- Pinheiro, J., Bates, D.M., 2006. Linear mixed-effects models: basic concepts and examples. Mix. Model. S S-PLUS 3–56. https://doi.org/10.1007/0-387-22747-4\_1.
- Plangoen, P., Babel, M.S., Clemente, R.S., Shrestha, S., Tripathi, N.K., 2013. Simulating the impact of future land use and climate change on soil erosion and deposition in the Mae Nam Nan sub-catchment. Thailand. Sustain. 5, 3244–3274. https://doi.org/ 10.3390/su5083244
- Puno, G.R., Marin, R.A., Puno, R.C.C., Toledo-Bruno, A.G., 2021. Geographic information system and process-based modeling of soil erosion and sediment yield in agricultural watershed. Glob. J. Environ. Sci. Manag. 7, 1–14. https://doi.org/10.22034/ giesm.2021.01.01.
- Qi, X., Qian, S., Chen, K., Li, J., Wu, X., Wang, Z., Deng, Z., Jiang, J., 2023. Dependence of daily precipitation and wind speed over coastal areas: evidence from China's coastline. Hydrol. Res. 54, 491–507. https://doi.org/10.2166/NH.2023.093.
- R Core Team, 2017. A Language and Environment for Statistical Computing [Software]. Version 4.3.1 (Beagle Scouts). R Core Team, Vienna, Austria. Available online: http://www.r-project.org (accessed on 10 November 2024).
- Renard, K.G., Freimund, J.R., 1994. Using monthly precipitation data to estimate the R-factor in the revised USLE. J. Hydrol. 157, 287–306. https://doi.org/10.1016/0022-1694(94)90110-4.
- Sakhraoui, F., 2023. Evaluation of the sensitivity of the RUSLE erosion model to rainfall erosivity: a case study of the Ksob watershed in central Algeria 23, 3262–3284. https://doi.org/10.2166/ws.2023.182.
- Saoud, M., Meddi, M., 2023. Estimation of soil erosion and sediment yield in Wadi El Hachem watershed (Algeria) using the RUSLE-SDR approach. J. Mt. Sci. 20, 367–380. https://doi.org/10.1007/s11629-022-7549-5.
- Sardari, M.R.A., Bazrafshan, O., Panagopoulos, T., Sardooi, E.R., 2019. Modeling the impact of climate change and land use change scenarios on soil erosion at the Minab dam watershed. Sustain 11. https://doi.org/10.3390/su10023353.
- dam watershed. Sustain 11. https://doi.org/10.3390/su10023353.

  Serbaji, M.M., Bouaziz, M., Weslati, O., 2023. Soil water Erosion modeling in Tunisia using RUSLE and GIS integrated approaches and geospatial data. Land 12. https://doi.org/10.3390/land12030548.
- Shi, W., Chen, T., Yang, J., Lou, Q., Liu, M., 2022. An improved MUSLE model incorporating the estimated runoff and peak discharge predicted sediment yield at the watershed scale on the Chinese loess plateau. J. Hydrol. 614, 128598. https:// doi.org/10.1016/j.ihydrol.2022.128598.
- Simonneaux, V., Cheggour, A., Deschamps, C., Mouillot, F., Cerdan, O., Le Bissonnais, Y., 2015. Land use and climate change effects on soil erosion in a semi-arid

- mountainous watershed (high atlas, Morocco). J. Arid Environ. 122, 64–75. https://doi.org/10.1016/j.jaridenv.2015.06.002.
- Sohoulande Djebou, D.C., Singh, V.P., 2016. Impact of climate change on precipitation patterns: a comparative approach. Int. J. Climatol. 36, 3588–3606. https://doi.org/ 10.1002/joc.4578.
- Souadi, Y., 2011. Université Du Québec À Montréal L 'Érosion Hydrique Au Maghreb Étude D 'Un Cas : Le Bassin Versant De L 'Oued Barbara (Tunisie Septentrionale)
- Tahiri, M., Tabyaoui, H., Hammichi, F. El, Achab, M., Tahiri, A., Hadi, H. El, 2017. Quantification de l'érosion hydrique et de la sédimentation à partir de modèles empiriques dans le bassin versant de Tahaddart (Rif nord occidental, Maroc)-Quantification of water erosion and sedimentation using empirical models in the Tahaddart watershed. Bull. l'Institut Sci. Rabat. Sect. Sci. la Terre 39, 87–101.
- Tsige, M.G., Malcherek, A., Seleshi, Y., 2022. Improving the modified universal soil loss equation by physical interpretation of its factors. Water (Switzerland) 14, 1–30. https://doi.org/10.3390/w14091450.
- Vavassori, A., Oxoli, D., Venuti, G., Brovelli, M.A., Siciliani de Cumis, M., Sacco, P., Tapete, D., 2024. A combined remote sensing and GIS-based method for local climate zone mapping using PRISMA and Sentinel-2 imagery. Int. J. Appl. Earth Obs. Geoinf. 131, 103944. https://doi.org/10.1016/j.jag.2024.103944.
- Vianney Nsabiyumva, J.M., Apollonio, C., Castelli, G., Petroselli, A., Sabir, M., Preti, F., 2023. Agricultural practices for hillslope Erosion mitigation: a case study in Morocco. Water (Switzerland) 15. https://doi.org/10.3390/w15112120.
- Werrell, C.E., Femia, F., 2017. The New Geostrategic Landscape of the Anthropocene. Wischmeier, W.H., Meyer, L.D., 1973. Soil erodibility on construction areas. Soil Eros. Causes Mech. Prev. Control 20–29.
- Wu, L., Liu, X., Ma, X. yi, 2018. Research progress on the watershed sediment delivery ratio. Int. J. Environ. Stud. 75, 565–579. https://doi.org/10.1080/ 00207233.2017.1392771
- Xiong, C., Tao, H., Liu, S., Liu, G., Wen, Z., Shang, Y., Wang, Q., Fang, C., Li, S., Song, K., 2024. Using satellite imagery to estimate CO2 partial pressure and exchange with the atmosphere in the Songhua River. J. Hydrol. 634, 131074. https://doi.org/ 10.1016/j.ihydrol.2024.131074.
- Xu, Z., Zhang, S., Hu, X., Zhou, Y., 2024. Construction of a monthly dynamic sediment delivery ratio model at the hillslope scale: a case study from a hilly loess region. Front. Environ. Sci. 12, 1–11. https://doi.org/10.3389/fenvs.2024.1341868.
- Yan, F., Wang, X., Huang, C., Zhang, J., Su, F., Zhao, Y., Lyne, V., 2023. Sea reclamation in mainland China: process, pattern, and management. Land use policy 127, 106555. https://doi.org/10.1016/j.landusepol.2023.106555.
- Yeneneh, N., Elias, E., Feyisa, G.L., 2022. Quantify soil erosion and sediment export in response to land use/cover change in the Suha watershed, northwestern highlands of Ethiopia: implications for watershed management. Environ. Syst. Res. 11. https:// doi.org/10.1186/s40068-022-00265-5.
- Yuan, K., Xu, H., Zhang, G., 2022. Is there spatial and temporal variability in the response of plant canopy and trunk growth to climate change in a typical River Basin of arid areas. Water (Switzerland) 14. https://doi.org/10.3390/w14101573.
- Zahnoun, A.A., Jamal, A.K., 2020. Estimation & Cartography the water Erosion by integration of the Gavrilovic "Epm" model using a Gis in the Mediterranean watershed: Oued Tleta (Western Rif, Morocco). Eur. J. Sci. Res. 155, 265–278.
- Zhang, W., Zhu, G., Zhao, L., Wang, L., Qiu, D., Ye, L., Lu, S., Lin, X., 2024. Quantifying the changes in solute transport caused by human influence on river connectivity in inland river basins. CATENA 246, 108360. https://doi.org/10.1016/j. catena 2024 108360
- Zhao, X.G., Shi, H., 2002. The change of the sediment delivery ratio from the slope and water-collected plot in the gully region of Loess Plateau. J. Mt. Sci. 20 (6), 718–722.